SYNTHESIS AND CHARACTERIZATION OF SUPERCONDUCTOR COMPOSITE $Bi_2Sr_2Ca_1Cu_2O_8$ /$La_{0.85}Sr_{0.15}MnO_3$

A thesis submitted in partial fulfillment for the award of degree in

Master of Science

in

PHYSICS

By

SHREELEKHA MISHRA

ROLL NO: 410PH2130

Under the Guidance of

Dr. Prakash Nath Vishwakarma

Department of Physics

National Institute of Technology, Rourkela

Rourkela-769008, Orissa, India

May-2012

DECLARATION

I hereby declare that the project work entitled "**Synthesis and characterization of superconductor composite $Bi_2Sr_2Ca_1Cu_2O_8/La_{0.85}Sr_{0.15}MnO_3$**" submitted to National Institute of Technology, Rourkela, is the record of an original work done by me under the guidance of Dr. Prakash NathVishwakarma, Assistant professor of NIT, Rourkela, and this project work has not performed the basis for the award of any degree or diploma/associate-ship/fellowship and similar project if any.

Shreelekha Mishra

Roll No-410ph2130

NIT, Rourkela

Department of Physics

National Institute of Technology

Rourkela-769008(Orissa)

CERTIFICATE

This is to certify that the thesis entitled "**Synthesis and characterization of superconductor composite $Bi_2Sr_2Ca_1Cu_2O_8/La_{0.85}Sr_{0.15}MnO_3$**" submitted by **Shreelekha Mishra** in partial fulfilment of the requirements for the award of degree of Master of Science in Physics at National Institute of Technology, Rourkela is an authentic work carried out by her under my supervision. To the best of my knowledge, the work done in this thesis has not been submitted by any other university/ Institute for the award of any degree or diploma.

Dr. Prakash Nath Vishwakarma

Date-

TABLE OF CONTENTS

DEDICATED TO MY PARENTS

ACKNOWLEDGEMENT

Apart from my efforts the success of this project depends largely on the encouragement and guide lines of many others. I take this opportunity to express my sincere gratitude to the people who have been instrumental in the successful completion of this project.

I would like to express my greatest appreciation to my guide Dr.Prakash Nath Vishwakarma for his valuable guidance and continuous support during my project, without whose encouragement and guidance this project would not have materialized.

I would like to give a sincere thanks to Miss Jashashree Ray, Mr.Achutya Ku.Biswal, and Miss Sanghamitra Acharya for their inspirative support throughout my project work, without which it would have been difficult .I also like to thank all the faculty members, PhD scholars, M Tech scholars and all member of department of physics NIT, Rourkela for their direct or indirect support towards the project.

For the generous support in the research of this project, I would like to acknowledge Department of Metallurgical and Material Science for the help in taking XRD and SEM.

I would like to give my heartfelt thanks to all my friends for their immense support and encouragement towards my project work.

I humbly prostrate myself before the Almighty for his grace and blessings, which enables me to complete this work smoothly.

Last but not least, I owe a special debt gratitude and love to my revered parents and all family members for their manual support, inspiration, strength, blessings and for everything.

Shreelekha Mishra

LIST OF FIGURES

ABSTRACT

Superconductor $Bi_2Sr_2Ca_1Cu_2O_8$ is prepared by solid state route and the substituent element $La_{0.85}Sr_{0.15}MnO_3$ is prepared by sol-gel combustion route. Then the composite of BSCCO(2212) with LSMO having different composition are prepared by solid state route. X-ray diffraction of BSCCO(2212) sintered at 880^0C for 12hrs and LSMO sintered at 820^0C for 5hrs are taken.The sharp and well defined peak of both BSCCO (2212)and LSMO is observed which shows the presence of the single phase having crystal structure tetragonal (a = 3.82 Å, b = 3.82 Å & c = 30.60 Å) and monoclinic (a = 5.48Å, b = 5.53 Å & c = 7.79 Å) for for BSCCO(2212) and LSMO respectively. In XRD pattern of compisites, some extra peaks are also observed. SEM analysisis done to know the morphology of BSCCO(2212) and its composites. EDXS analysis revels exact constituent of the different element free from the other element. Resistivity vs temperature measurement is done for all the sample. The T_c of the sample was found to be 74.91K and for the other composition of LSMO added BSCCO(2212) the T_c value gradually decreases which indicates the decrement in the transition peak and the disorderness of the sample.

CHAPTER-1

INTRODUCTION

Superconductivity was discovered in 1911 by Dutch physicist Heike Kammerlingh Onnes by studying the resistivity of solid mercury at cryogenic temperatures using the recently-discovered liquid helium as a refrigerant. After this discovery of superconductivity many metals and alloys had shown superconductivity when these specimen are cooled to sufficiently low temperature.

Superconducting materials are very important in scientific and technological prospective. Some technological innovations benefiting from the discovery of superconductivity are

- Magnetic resonance imaging
- Sensitive magnetometer based on SQUIDS.
- Beam-steering magnets in particle accelerator.
- Microwave filters.
- Electronic power transmission cables.
- Magnetic levitation devices.

1.1HISTORY

In the history of superconductivity few important milestones are

- ✓ In 1911 Dutch physicist Heike Kammerlingh Onnes by studying the resistivity of solid mercury at cryogenic temperatures using the liquid helium as a refrigerant discovered superconductivity.
- ✓ In1933 the basic physics for the understanding of superconductivity was developed by Meissner and Ochsenfeld, called Meissner effect.
- ✓ In 1950, Ginzburg-Landau develop a theory known as Ginzburg-Landau theory to explain the microscopic properties of superconductors.
- ✓ In the same year, Maxwell and Reynolds et.al. found the critical temperature dependence relation with the isotopic mass of the constituent element.
- ✓ The complete microscopic theory of superconductivity was finally proposed in 1957 by Barden, Cooper and Schrieffer by their theory known as BCS theory.

- ✓ A new era in the study of superconductivity began in 1986 with the discovery of high critical temperature superconductor and introduced the outstanding challenges of theoretical condensed matter physics.[1]

1.2PROPERTIES OF SUPERCONDUCTORS

1.2.1 ELECTROMAGNETIC PROPERTIES

(a) Meissner effect or Diamagnetism

The complete ejection of magnetic flux from the specimen when they are cooled through the transition temperature in a magnetic field is known as Meissner's effect. The applied magnetic field, below transition temperature, get to magnetize the substance in an opposite direction, so it shows a negative magnetic susceptibility. Since there is complete expulsion of magnetic flux, so superconductors are perfectly diamagnetic. [2, 3]

$$\chi = \frac{M}{H} = -1$$

Where, H=strength of the field

M=magnetisation or intensity of magnetisation

χ is susceptibility of the material

.

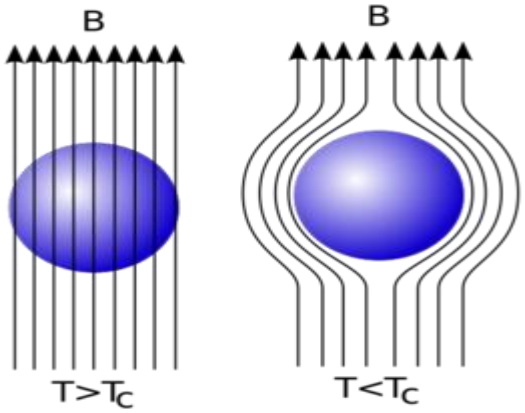

Fig1.1 Meissner Effect in Superconducting Sphere [2]

(b) Critical field

The value of the magnetic field at which the superconductivity vanishes is called the critical field, H_c[2]. In superconductors, their normal resistance may be restored if a magnetic field greater than the critical value; Hc is applied to the specimen. H_c depends on the nature of material and also with the critical temperature(T_c).At critical temperature the critical field is zero and the critical field at any temperature below the critical temperature is calculated from the relation,

$$H_C = H_C(0)[1-(\frac{T}{T_C})^2]$$

Here, H_c=maximum critical field strength at temperature T.

H_c (0) =maximum critical field strength occurring at absolute zero.

In general for higher value of Hc, the T_c value is lower and vice versa.

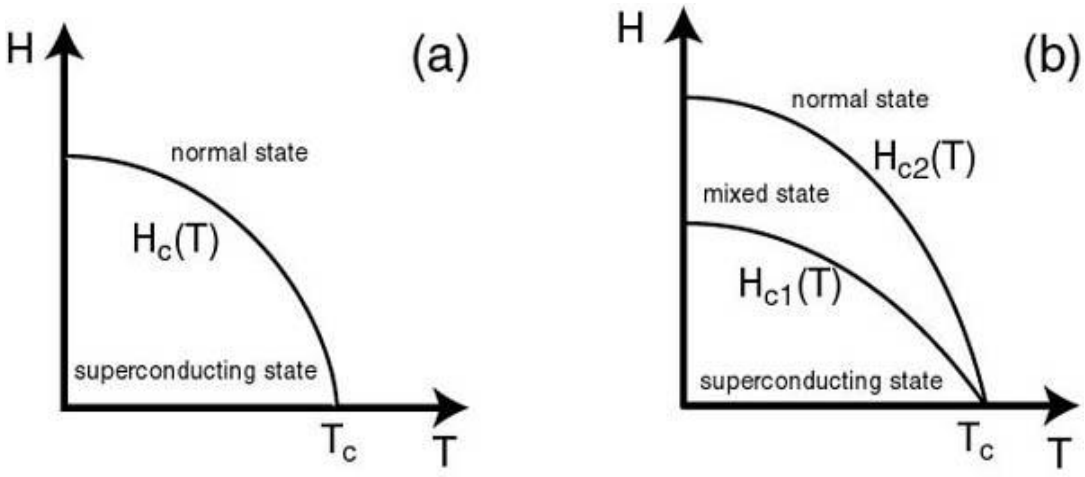

Fig1.2 Magnetic phase diagram of (a) type I Superconductor and (b) type II superconductor [4]

(c)Critical current

The minimum current for which the super conductivity retains in the sample is called the critical current I_c [2]. Hence if a superconductor carries a current such that the field which it produces is H_c, then the resistance of the sample is restored or the material becomes normal. The critical current I_c will decrease linearly with increase of applied field upto zero.

(d)Flux quantization

London, in 1950, speculated that magnetic flux penetrating through a superconducting ring or a hollow superconducting cylinder can have values equal to nh/e, where n is an integer. The flux quantization has been confirmed experimentally, but the quantum of flux has been found to be h/2e rather than h/e .This unit of flux is called a fluxoid.[2-3]

(e) Josephson Effect

Josephson observed some remarkable effects associated with the tunnelling of superconducting electrons through a very thin insulator (1-5 nm) sandwiched between two superconductors. Such an insulating layer forms a weak link between the superconductors which is referred to as the Josephson junction.

(i)The dc Josephson Effect: A dc current flows across the junction without any application of voltage.

(ii)The ac Josephson Effect: An application of rf voltage along with the dc voltage can result in the flow of direct current through the junction. Hence this effect has been utilized to measure e/h very precisely and may be used as a means of establishing a voltage standard [2, 3].

1.2.2 THERMAL PROPERTIES

(a)Entropy

A marked decrease in entropy is observed during normal to superconductivity transition near the critical temperature; which indicates that the superconducting state is more ordered than normal state. [3]

(b)Specific heat

From the specific heat study of superconductor we can get the information about the existence of the band gap in superconductors [3]. As we know specific heat of normal metal,

$$\mathbf{C_n = \gamma T + \beta T^3}$$

Where, γT=specific heat term

βT^3=contribution of lattice vibration at low temp.

Specific heat of superconductor shows a jump at T_c since the superconductivity affects electron mainly. So, the lattice vibration part remains unaffected. By this substitution the electronic specific heat C_{es} shows the exponential curve.

$$\mathbf{C_{es}(T) = Aexp(-\frac{\Delta}{Tk_\beta})}$$

and this indicates the existence of finite gap in the superconductor.

(c)Isotope effect

In the year 1950 the dependence of transition temperature of superconductor with its isotopic mass M was given, i.e.

$$\mathbf{T_c \propto M^{-1/2}}$$

The Debye temperature, θ_D of the phonon spectrum is related to M as,

$$\mathbf{\theta_D M^{1/2} = constant}$$

$$\mathbf{T_c \propto \theta_D \propto M^{-1/2}}$$

This sign indicates that the lattice vibration or the electron- phonon interaction plays an important role for the occurrence of superconductivity and this prediction gives the idea that two electrons in a metal can effectively attract each other, and this attraction is mediated by lattice vibration. [3]

1.2.3 BCS THEORY

The understanding of superconductivity was advanced in 1957 by three American physicists John Bardeen, Leon Cooper and Robert Schrieffer, through a theory known as BCS theory. The BCS theory explains superconductivity at temperature close to absolute zero. A key conceptual element in this theory is the pairing of electrons by special type of attraction close to the Fermi level. These pair of electrons is called Cooper pairs and they formed through interaction within the cryptal lattice. The idea is if we consider an electron passing close to an ion, there will be a momentary attraction between them and due to this the ion is set in motion and consequently distorts the lattices. This in turn could interact with a second electron nearby which will also be attracted to the ion. Thus we interpret that the two electrons interact via the lattice distortion or the phonon field resulting in the lowering of

electron energy implies that the force between the two electrons is attractive. This type of interaction is called electron-lattice- electron interaction. [2, 4, 6]

The BCS theory is able to explain all the properties shown by the superconductor.

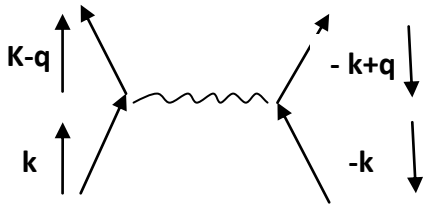

Fig1.3 Electron-phonon –Electron interaction. [3]

1.2.4 COHERENCE LENGTH

One of the characteristic lengths for the description of superconductor is called the coherence length. It interprets the approximate size of the cooper pair. It can be defined as; the maximum distance up to which the states of pair electron are correlated to produce superconductivity is called coherence length ε_0. It is related to the Fermi velocity for the material and the energy gap associated with the condensation to the superconducting state. [4, 7, 8]

The superconductivity coherence length is given by

$$\in = \frac{-2\mathbf{h}\mathbf{V_f}}{\pi\Delta}$$

Where, h is the reduced plank constant, m is the mass of the cooper pair, v_f is the velocity of cooper pair, Δ is superconducting energy gap.

1.2.5 PENETRATION DEPTH

In 1935 F. London and H. London described the Meissner effect and zero resistivity of the superconducting material by taking E=0 and B=0 in the Maxwell's electromagnetic equation. [4, 7]. According to this the applied field does not suddenly drop to zero at the surface of the Superconductor but decay ex potentially according to the equation.

$$\boldsymbol{B(x) = B_0 \exp(-x/\lambda_L)}$$

In superconductor, the London penetration depth , λ_L characterizes the distance to which a magnetic field penetrates into a superconductor and become equal to 1/e times that of the magnetic field at the surface of the superconductor and is given by,

$$\boldsymbol{\epsilon_0 = (\frac{\epsilon_0 c^2 m}{ne^2})^{1/2}}$$

Where, λ_L can be distance across in which the magnetic field becomes 'e' times weaker

n = superconducting electron density

The ratio of London penetration depth to the coherence length is

$$\mathbf{k = \frac{\lambda}{\epsilon_0}}$$

is a number and changes in value from type I to type II superconductor.

For type I superconductor $k<1/\sqrt{2}$ and type II superconductor $k>1/\sqrt{2}$

1.3 CLASSIFICATION OF SUPERCONDUCTORS

1.3.1 By magnetic response

According to their response to magnetic field they are classified into two types.

Type I superconductors-They have a single critical field and above which the material become normal. They are pure and easily give away their superconductivity at lower field strength so referred as known as soft super conductors. [3, 5]

Type II superconductors -They have two critical field. It follows from the graph that for field less than H_{c1}, the material exhibit perfect diamagnetism and the flux penetration does not takes place. Thus for $H<H_{c1}$ the material exhibit in the superconducting state. If the field more than H_{c1} is pass through the specimen, the flux begins to penetrate the specimen and for H=Hc, the complete penetration occurs and the material become a normal conductor. As relatively large field are needed to bring these superconductor to normal state, so they are also called as hard superconductors [3, 5].

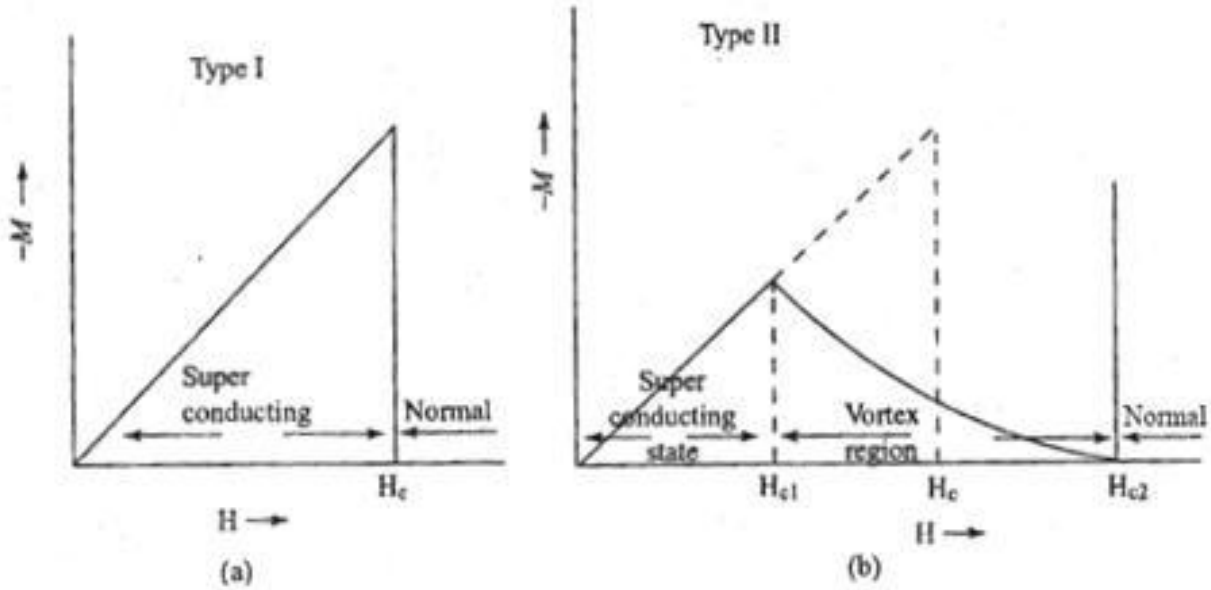

Fig1.4(a) Type I and (b)TypeII superconductor [2]

1.3.2 By theory

According to the response of BCS theory they are classified as [5]

I. Conventional- They are explained by BCS theory, generally having low T_c, hence called as low T_c superconductor.

II. Unconventional-They do not follow BCS theory. They show high T_c than the conventional superconductor, so generally known as high T_c superconductor.

1.3.3 By material

I. Chemical elements (e.g.-mercury, lead etc.)

II. Alloys(niobium, titanium or germanium-niobium)

III. Ceramics(YBCO, magnesium diboride)

IV. Organic superconductors (Fullerenes, carbon nanotubes etc.)

1.4 HIGH T_c SUPERCONDUCTORS

The history of high T_c superconductors was begins in 1986 with the discovery of superconductors on the system Ba-La-Cu-O having the critical temperature 36k by Karl Muller and Johannes Bednorz in IBM research laboratory. This opened a new branch of high T_c superconductivity namely "High T_c superconductivity "as they broke the barrier of 30K imposed by BCS theory. Soon after this many other oxide based superconductors were discovered having the critical temperature greater than 90K and they are shown below with the discovery year and their respective T_c in fig 1.5

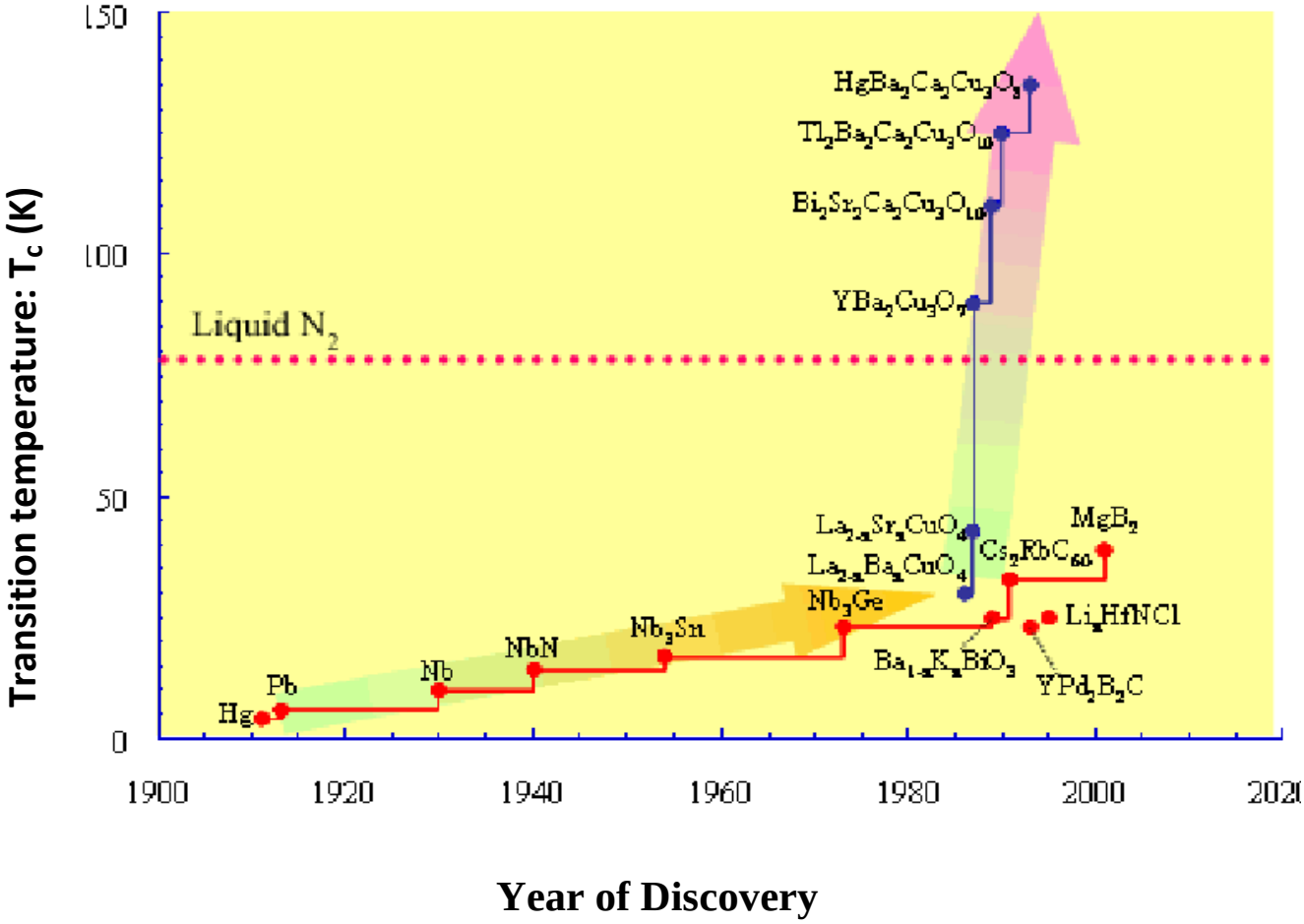

Fig1.5 History of superconductivity [9]

They have their structure derived from ideal Perovskite structure [9](therefore termed as defect perovskite structure), either through an intergrowth phenomenon or by an ordered removal of oxygen atoms. They have layered crystal structure consisting of one or more

CuO_2 layers. Copper is present in the mixed state involving a partial oxidation of Cu^{2+} to Cu^{3+}. There is a charge transfer to and from the CuO_2 layers which is induced by doping near the metal insulator phase existing in all oxide high T_c superconductors. [9]

LBCO: LBCO (Lanthanum Barium Copper Oxide) is the first oxide based HTSC material developed in 1986 having T_c of 35K. It is the only insulating material in the HTSC family. This discovery shows the path for the additional research in high T_c superconductivity on cuprate materials with structure similar to LBCO. [10]

YBCO: YBCO (Yttrium Barium Copper Oxide) is the first material to break the liquid nitrogen temperature (77 K). It was discovered in the year 1987 by Paul Chu in the University of Houston. It shows the highest T_c of 93 K. YBCO is highly studied as it is the cleanest and most ordered crystals and shows strong electron-electron interaction.[11]

BSCCO: BSCCO (Bismuth Strontium Calcium Copper Oxide) was the first high temperature superconductor which did not contain a rare earth element. It is a cuprate superconductor which shares a two dimensional layered Perovskite structure with the superconducting copper oxide plane. It has general formula $Bi_2Sr_2Ca_{n-1}Cu_nO_{2n+4+x}$ with specific transition temperature ranging from T_c=20 K(n=1, 2201 phase), 85 K(n=2, 2212 phase), 110 K(n=3,2223 phase) and 104 K(n=4,2224 phase)[12].

TBCCO: It is the next higher member of HTSC family. It was discovered in the same year as BSCCO. General formula of TBCCO (Thallium Barium Calcium Copper Oxide) is $Ti_2Ba_2Ca_{n-1}Cu_nO_{2n+4+x}$ with transition temperature ranging from T_c=85 K (n=1, 2201 phase), 110 K(n=2, 2212 phase) and 127 K(n=3,2223 phase). The CuO_2 layers are thicker and closer together in comparison to BSCCO system.

HBCCO: HBCCO (Mercury Barium Calcium Copper Oxide) is the highest member of HTSC family till today. It was discovered in 2009. General formula of HBCCO system is $Hg_1Ba_2Ca_{n-1}Cu_nO_{2n+2+x}$ with specific transition temperature ranging from T_c=94 K (n=1, 1201 phase), 128 K (n=2, 1212 phase) and 134 K (n=3, 1223 phase). The T_c of the Hg compound containing one CuO_2 layer is much larger as compared to the one CuO_2 layer compounds of TBCCO.

Recently the iron based superconductors have been discovered that shows the T_c above 56 K. The first iron based superconductor was developed by Ramihar et.al on 23rd February on

LaFeAsO system. These are the first non-cuprate material where the two dimensional electronic structure was shown and their T_c is also controlled by a systematic aliovalent ion doping into the insulating block layers.

1.5 APPLICATION OF HIGH T_c SUPERCONDUCTORS

- As HTS thin film shows excellent superconducting properties (i.e. T_c >90, J_c (at 77K, 0T)>10^6A/Cm^2, so they are useful for superconductive electronics. They are used in commercial and military microwave filter systems.
- For better rejection of interference noise in aircraft radar system, HTS filters are used in aircraft electronics.
- In rural areas rf coverage can be achieved by small number of base station, by use of HTS filters the rf power of the handsets in urban areas can be reduced.
- HTS Josephson junctions are available which can be used for the construction of highly sensitive magnetic field sensors (SQUIDS) and only HTS SQUIDS are able to observe magnetic signals in the presence of disturbing background fields without the burden of magnetic shielding. Also the SQUIDS fabricated by the HTS are applicable in medical diagnostics, sea communication, sub marine detection and geographical prospecting.
- As the HTS on superconducting magnet reduce the heat load to the cold magnetic system, so they are used in many application where classical superconducting coils cannot be used.
- A magnetically levitated train is developed in China by using HTS. The mechanism behind this is the magnet induced currents in the rails, causing a repulsion which suspends the train above the track.
- High gradient separation or HTS magnetic separators can be designed with HTS wires and cooled with two stage G-M cryocooler.
- High voltage generator can be developed by using HTS inductor and electronic RCL series resonant circuit.[13,14]

1.6 WHY BSCCO

As the high temperature superconductors slows the emerging application in various field and is most recent and BSCCO is the widest among this due to its unique properties. BSCCO is the important category of high temperature superconductors which did not contain rare earth

element and shares a two dimensional layered (perovskite) structure where the superconducting phenomenon varies in copper oxide plane. It gives the high T_c value and shows more stability in superconducting behaviour w.r.to oxygen loss in comparison to YBCO. BSCCO compounds exhibit both an intrinsic Josephson effect and anisotropic (dimensional) behaviour. [15] BSCCO is generally categorized into three different structures according to their 'n' values. There are, T_c=20K (n=1, 2201), T_c=95K (n=2, 2212), T_c=110K (n=3, 2223)

The below figure shows the crystallographic unit cell of three different structure.

1.6.1 CRYSTAL STRUCTURE OF BSCCO

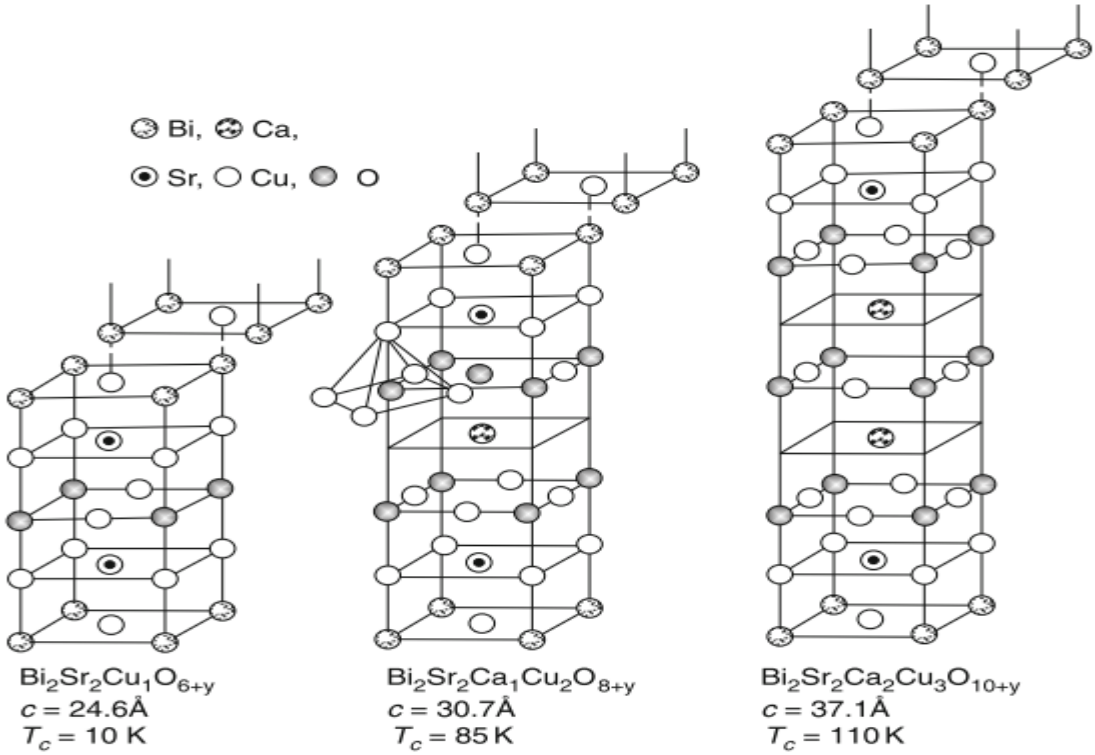

Fig 1.6 Crystal structure of BSCCO family

The crystallographic unit cell of BSCCO structure contains three layers. They are "Reservoir layer"(i.e. SrO and BiO layer) that reserves the electron ,just above it contains superconducting layer(i.e. CuO)in this layer the doping can be possible to vary the property of the superconductors , above this it contains Insulating layer(CaO and CuO),where CaO

and CuO plane form the Josephson junction between them. Though BSCCO structure are almost same, BSCCO 2212 comprises two repeating units whereas BSCCO-2201 has one less CuO_2 in its top and bottom half and no Ca layer , while BSCCO-2223 has an extra CuO_2 and Ca layer in each half.[12]

In our synthesis we prefer BSCCO 2212 phase as its T_c is considerably high and it is easy to synthesis as they are thermodynamically stable over a wide range of temperature and within the stoichiometric range, as compared to 2223 phase [16].

The layer structure of BSCCO(2212) superconducting single crystal are natural stacks of superconductor-insulator superconductor multifunction, are called Intrinsic Josephson junction(IJJ).Due to large anisotropic structural and electrical properties it considered as the important source for superconductivity and device application. IJJ's can be used to generate tetrahartz radiation that has potential application areas in material characterisation, biology, communication, medicine and security. Recently, strong, continuous and monochromatic THZ radiation was generated by single crystal of 2212 IJJ [17]

As it is easily melt processed to form highly texture material that provides uniform superconducting current distribution along conductors such as silver sheeted tapes, wires and long roads so it shows the promising application [18]

1.7 MOTIVATION (FOR PREPARATION OF COMPOSITE)

Superconductors are diamagnetic, hence completely repels magnetic lines of force until magnetic field HC_1.If the magnetic field is increased further, magnetic flux starts penetrating into the superconductor in the form of vertices. With further increase in field strength more number of magnetic fields penetrates into it until HC_2, beyond which all lines of force penetrate, i.e., normal region.

When a magnetic field penetrate into the superconducting region, it creates an electric field. In the presence of both electric and magnetic field vertices experience Lorentz force, i.e., $F_L = J \times \frac{B}{C}$, where J is the amount of current in the sample, B is the magnetic field and C is an arbitrary constant. So vertices start to flow in mixed state region. When flux lines flows it experiences viscous drag force F_v which opposes this motion i.e., ηV_L inside the medium, where V_L vertex velocity and η proportionality constant. The driving force is balanced by viscous force per unit length of vortex line. In the absence of pinning

$$J \times \frac{B}{C} = \eta V_L$$

$$\text{i.e.} \quad F_L = j \times \frac{B}{C} - \eta V_L = 0$$

When the Lorentz force (F_L) overcomes the viscous force (F_v) at higher magnetic field, the vortex or flux lines starts moving, as the vertices move, resistance increases so, critical current density (J_c) decreases. For a practical application point of view we have to stop the vertex movement, thereby enhancement of J_c by introducing some form of pinning force. This pinning force is introduced trough the addition of pinning centres or defects that act to add a potential well where the vertices will become pinned. Pinning comes in the form of any inhomogeneity in the material such as, impurities, grain boundaries or voids. These voids can be introduced through doping and impurities.

High temperature superconductor (HTSC) of granular shapes have grain boundary. Superconductivity originates inside the grain boundary acts like pinning centres and prevents vortex motion. By addition of suitable microscopic impurity to the HTSC.

So composite of nano particles of metal, insulator and oxides are very interesting in HTSC for creating pinning centres. From the literature, it is concluded that out of all, magnetic nano inclusion are more suitable to enhance J_c. As LSMO acts as half metal and act as a good barrier layers in superconducting-ferromagnetic-superconducting heterostructure, so it is useful for effective pinning centre.

As in above we discuss about the various application of BSCCO but the pinning magnetic flux line in anisotropic high Tc superconductor is an area of active research. Generally BSCCO (2212) materials are applied for tapes by which high field magnets worked at low temperature, but this cannot be useful in high temperature and high field region. The major limitation of polycrystalline Bi-based superconductor are the weak flux pinning and weak links in granular networks at relatively high temperature and applied magnetic field, these can be overcome by finding the effective pinning centres that are introduced into the material by the addition of various nano particles and make them useful for commercial applications.

Now we see how the different nano particles effect on the microstructure and pinning property of the BSCCO (2212).

1.8 LITERATURE SURVEY

Different nano-particles effect on the microstructure and pinning property of BSCCO (2212)

(1) The effect of nano sized MgO powder addition to Bi (2212) in the weight ratio 95:5 will change the T_c and also the J_c. It was reported that the T_c of the Bi (2212) single crystal was 93K but it decreases to 92K after doping. J_c also increases by the addition of nano particles MgO but the sufficient enhancement of J_c has not yet been achieved. In case of high T_c superconductor, the irreversibility field B_{irr} has been taken as the appropriate scaling field instead of the upper critical field Bc_2. The addition of MgO nano particles to Bi (2212) improve B_{irr} and F_p (pinning force density) and also improves the flux creep property.[19]

(2) The investigation of nano sized NiO addition on the phase formation and flux pinning of the polycrystalline dual phase i.e. BSCCO(2223) and BSCCO(2212) in $(BSCCO)_{1-x}$ $(NiO)_x$ composition should be taken with x (0.000 to0.005). It shows that with increase of x the volume fraction of the high critical temperature phase 2223 decreases gradually with increase in the relatively low T_c phase (2212). From the XRD analysis it was observed that slight increase in the 'c' lattice parameter with almost no change in 'a' and 'b' due to nano NiO addition. Vortex. Pinning forces were found to be suppressed by these NiO nano particles [20]

(3) The effect of Ni substitution on the properties of Bi-based superconductor with (x= (Ni) =0, 0.05, 0.1, 0.2) were investigated by various characterizing technique and it has been found that the T_c does not change independently on Ni content. But J_c decreases with increasing Ni substitution.[21]

(4) By increasing the extra calcium and copper content in the starting material of Bi-Sr-Ca-Cu-O results in the enhancement of the intragrain critical current density (J_c) 30 times w.r.to the undoped sample. [22]

(5) Addition of perovskites $SrAO_3$(A=Zr,Sr etc.) with Bi-2212 matrix, shows the partial incorporation of the particles into Bi-2212 grains and partially agglomerated, forming the thin closed areas between the Bi-2212 lamellas and due to this the J_c increases and T_c decreases [23]

So, from the above literature we can conclude that the considerable enhancement in J_c has been achieved by the introduction of high concentration of pinning centres such as crystalline defects etc. and we observed that almost by all nano particle substitution to BSCCO(2212) the critical current density increases and critical temperature decreases with higher concentration of the nano particles. In our experiment we take LSMO as nano particle with BSCCO and show the variation in T_c with different concentration of the LSMO has been discussed in the result and discussion section.

CHAPTER-2

SYNTHESIS OF SAMPLES

2.1 METHODS OF PREPARATION (BSCCO)

Synthesis of the sample in single phase is the most important part of the research work. According to the literature survey, various methods have been adopted for the preparation of BSCCO- 2212. These are decarbonation, solid state synthesis route, chemical precipitation, melt process, spray pyrolysis, sol-gel synthesis route, etc.

(1) The sample is prepared by decarbonation reaction by taking $CaCO_3$, $SrCO_3$, Bi_2O_3 and CuO with 99% purity as starting material. They are mixed in the stoichiometric ratio and sintered at 940^oC for 48 hour [24]

(2) The sample has been prepared by the solid state method by taking $CaCO_3$,$SrCO_3$,Bi_2O_3 and CuO as starting precursors and mixed in appropriate amount with a Bi:Sr:Ca:Cu cation ratio of 2:2:1:2 and finally grinded the resultant mixture was heated for 96 hour at 850^oC under air with two intermediate grinding [25]

(3) The sample has been prepared by chemical precipitation technique. In this technique the starting solution was prepared by dissolving Bi_2O_3, SrCO3, CaCO3 and Cu $(NO_3)_2$ in dilute nitric acid. The pH has to be maintained about 0.5 during mixing. The ions are precipitated from the solution as hydroxyl-carbonates by the using the mixture of tetra methyl ammonium hydroxide (TMAOH) and tetra methyl ammonium carbonate as the precipitating agent. The precipitate is dried a temperature between 400-500^o C, then the power was calcined at 750^oC at reduced pressure of 3 Torr in flow of oxygen for 6-10 hour followed by the ambient pressure in CO_2 ,with 800-840^oC temperature for 24 hours (without air) [26]

(4) The sample was prepared by melt process by two different ways .In both the cases Bi_2O_3,SrO,CaO and CuO are taken as starting material and mixed in desired composition 2:2:1:2. Then it was taken in alumina crucible and heated at temperature between 1000 -1100^oC upto the molten state. The melt are taken in copper moulds and slowly cooled to room temperature. Then the two routes of treatment were followed up. [27]

(5) The material was prepared by solid state reaction method. $CaCO_3$, $SrCO_3$, Bi_2O_3 and CuO with high purity i.e., 99.90% were mixed, pressed and then sintered in air at 860^oC for two or more days then quenched to room temperature[28]

a) Annealing in air has been done by heating the melt to 815^oC at the rate of 30^oC per hour, holding at 815^oC for 12-60 hour depending upon the size and then pulled at the rate of 20^oC per hour.
b) Same annealing procedure carried out with the solidified melt in powder form

(6) The superconducting films of Bismuth strontium cuprate were prepared by spray pyrolysis. For this method the nitrate stock solution of 0.5 molar for Bi_2O_3, $SrCO_3$, $CaCO_3$ and Cu were prepared dissolution in minimal amount nitric acid (0,25N). Then the solution were sprayed onto (100) oriented $SrTiO_3$ substrate heated at $500\text{-}550^oC$. Then the 10 min annealing in dry air at $800\text{-}890^oC$ followed by slow cooling in dry air (2.5-3 hour at 300^oC[29]

(7) The sample was prepared by solid state route with starting material $SrCO_3$, $CaCO_3$ and CuO in the atomic ratio Sr: Ca: Cu=2:1:2 .The metal was heated at900^0c for 24 hours with intermediate grinding. Then Bi_2O_3 was added to this to get a mixture in the atomic ratio Br: Sr: Ca: Cu=2:2:1:2.The prepared powder is sintered in air at 850^0cfor 16 hrs and slowly cooled.[30]

2.2 INFERENCE DRAWN FOR BSCCO SYNTHESIS

From the above mentioned methods, solid state synthesis route is found most convenient and gives nearly the single phase. More over there is no loss of the sample where as in sol-gel process; the sample is highly porous and produces contraction on sintering. In general the advantage of solid state route over all other synthesis route are (1) it give better homogeneity (2) higher yields of desired product (3) easy to prepare.[31,32]

Hence the solid state synthesis is chosen for the preparation of the sample.

2.3 SYNTHESIS OF BSCCO

The sample is prepared by solid state synthesis route. Bi_2O_3, $SrCO_3$, $CaCO_3$ and CuO powder is taken in the ratio Bi: Sr: Ca: Cu in 2:2:1:2 and grinded for 3 hours in an agate mortar. The powder is then put in the furnace at 700^oC for 12 hour and allowed to cool naturally. It is then taken out and grinded for 3 hours and again put in the furnace at 770^oC for 12 hours. After that the same grinding process is repeated and the sample is put in the furnace for calcination at 820^oC for 20 hours. Finally the sample is pressed into pellet of 10mm diameter and 5mm thickness by dry pressing method and sintered at 880^oC for 12 hours. The obtained sample is then characterized by resistivity, x-ray diffraction SEM, EDXS.

FLOW CHART FOR BSCCO SYNTHESIS

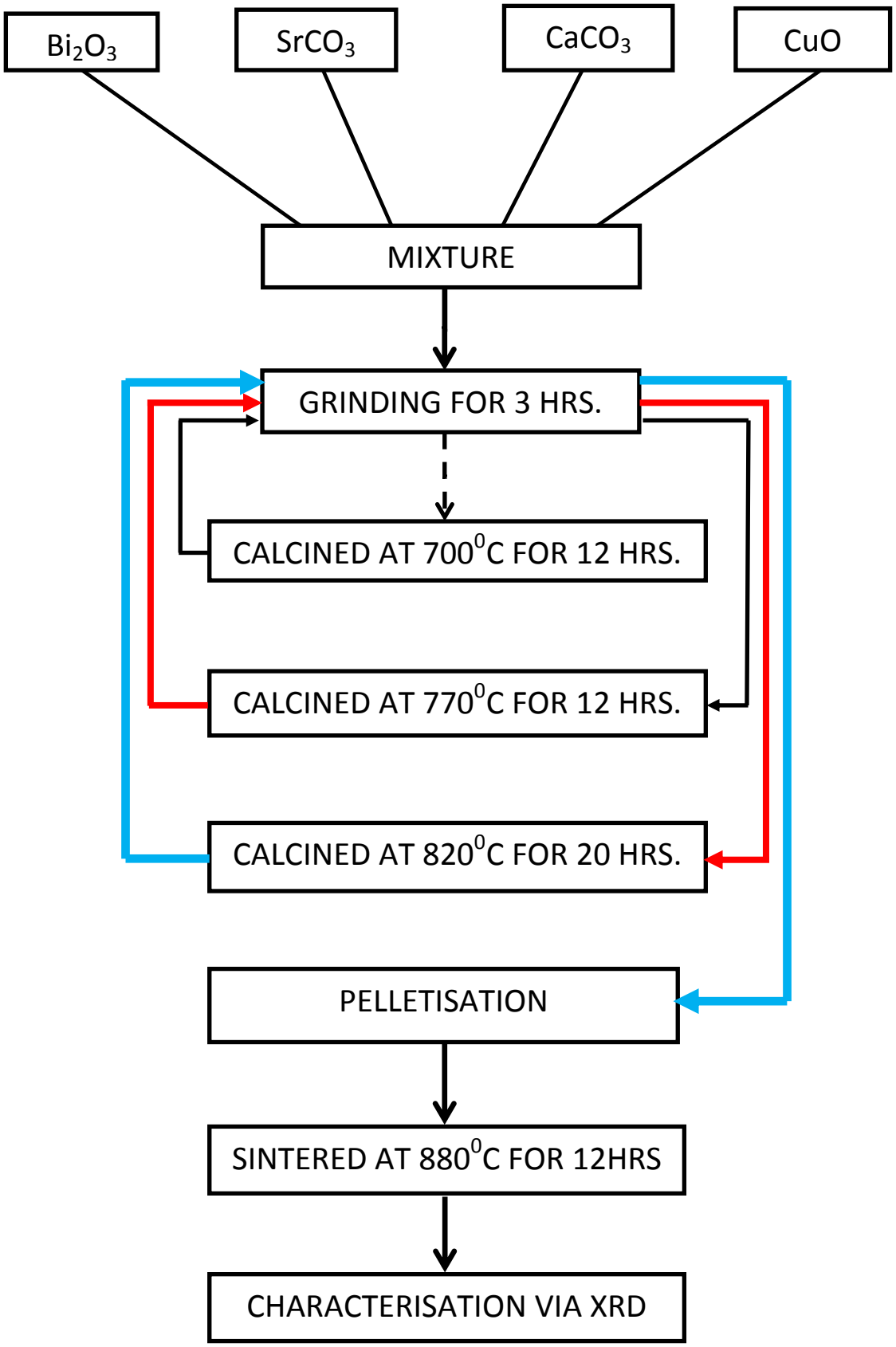

SYNTHESIS OF LSMO

2.4 CHOICE OF SAMPLE

Lanthanum manganite ($LaMnO_3$) is an antiferromagnetic insulator which when doped with strontium; undergo metal–insulator transition and ferro-paramagnetic transition at T_c and T_p respectively. Strontium doped lanthanum manganite (LSMO) is an oxide ceramic material with general formula ($La_{1-x}Sr_x\ MnO_3$), where 'x' describes the doping level of strontium. It has perovskite structure; of the form ABO_3 with Lanthanum and strontium occupying the A-site position (corner of a cube) and Mn occupy B-site position (body centre of a cube) and all the face centred position are occupied by oxygen.[33,34,35,36]

2.5 PROPERTIES OF LSMO

LSMO are half metals with manganese configuration Mn^{+3}, while Mn^{+4} give rise to a metallic state with a negligible spin polarisation at the Fermi level. The electronic property of LSMO is described by band theory which reflects the half-metallic behaviour. Below the Curie temperature LSMO behaves as a metal (from electrical point of view) and as ferromagnet (from magnetic point of view). Due to this property LSMO is use as a "barrier" layers in high Tc superconductors. [37, 38]

2.6 APPLICATION OF LSMO

1. LSMO is Manganese-based pervoskite oxide and they show colossal magneto resistance (CMR) property that enables them to dramatically change their electrical resistance in the presence of magnetic field. As they show very large magneto resistance, so they can be used in magnetic sensors. Read heads for magnetic recording devices are one of the most interesting applications of the magnetoresistance. [39,40]
2. Due to its half-metallic behaviour i.e. they change their property according to spin orientation and which make them useful in spintronics devices. It is a new approach to electronics which makes use of the spin of the carriers as well as their charge .So, the devices formed by this are smaller, denser, and can store information that can be

processed by manipulating the spin of electrons. It can be used in microelectronics. [40]

3. They are commonly used as cathode material in commercially produced solid oxide fuel cells (SOFCs), because of their high electrical conductivity at higher temperatures. [39]
4. LSMO motors having power ranges from 0.55-11 kW and it is use in machine tools in wet environment to ensure reliable operation in difficult conditions, with improving manufacturing productivity. [41]
5. LSMO show high T_c value (about 360 K) and a large magnetic moment at room temperature. So it is use in Hyperthermia application in which the magnetic nano particles of fairly uniform size, having Curie temperature above room temperature is required. It shows large application in biomedical field as they do not change their properties like Curie temperature at 360K after conjugation with biomolecules. [42]

6. The figure (2.1) shows the temperature dependence with resistivity for LSMO. It does not indicate any ferromagnetic transition for concentration $x \leq 0.05$.It shows a non-metallic behaviour for $x \leq 0.2$.With the increase in 'x' it shows metallic behaviour with shifting of T_c towards high temperature. [43]

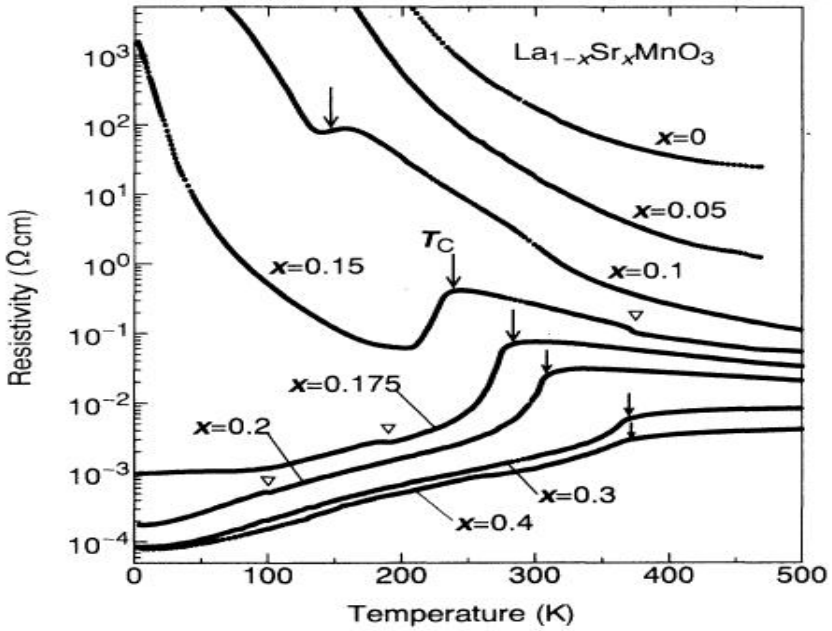

Fig2.1 Temperature dependence of resistivity for LSMO crystal [43]

2.7 LSMO PREPARATION METHODS

Some of the conventional method of LSMO preparations is:

(1) Sol-gel soft chemical method [44]

(2) Solid state method [45]

(3) Pulse laser deposition method [46]

(4) Metal organic deposition technique [47]

(5) Carbonate precipitation route [48]

(6) Floating zone method [49]

(7) Spray dryer method [45]

2.8INFERENCE FOR LSMO SYNTHESIS

Out of all synthesis routes, the sol-gel route is found to result nearly single phase. In liquid phase, the constituents are mixed at the atomic level and then the lattice growth occurs. Another advantage of sol-gel combustion synthesis is that the chance of impurity is lesser and the small grain size particle can be prepared. So the sol-gel combustion synthesis is chosen for the preparation of the sample.

2.9 SYNTHESIS OF LSMO

The compound $La_{0.85}Sr_{0.15}MnO_3$ is prepared by sol-gel combustion route. Manganese carbonate ($MnCO_3$), Lanthanum nitrate ($LaNO_3$), Strontium nitrate ($Sr(NO_3)_2$) are chosen as the precursors for the synthesis. Glycine is chosen as the fuel for the synthesis. At first a starting solution of $MnCO_3$ is made by mixing with nitric acid (15ml) and then with water (10ml). Then $La(NO_3)_3$ and $Sr(NO_3)_2$ are taken in stoichiometric ratio and dissolved in

distilled water. All the solutions are added to the chelating agent (glycine) in stoichiometric proportion (metal nitrate: glycine=1:1). The colour of the sample is found to be light brown. A continuous slow heating with stirring is maintained over hot plate throughout the experiment. After 4-5 hours, gel is formed without any precipitation due to the evaporation of water. The light brown colour solution changes to the deep brown colour. After 30 min powder is obtained with vigorous reaction and the gel burnt to form black powered. The powder so obtained is then grinded for 2 hours and then calcined for 5 hours at temperature $820^{o}C$ where the furnace heating rate is maintained at 5^{o}/min. After cooling to room temperature, the sample is collected from the furnace and used for necessary characterization.

FLOW CHART FOR LSMO SYNTHESIS

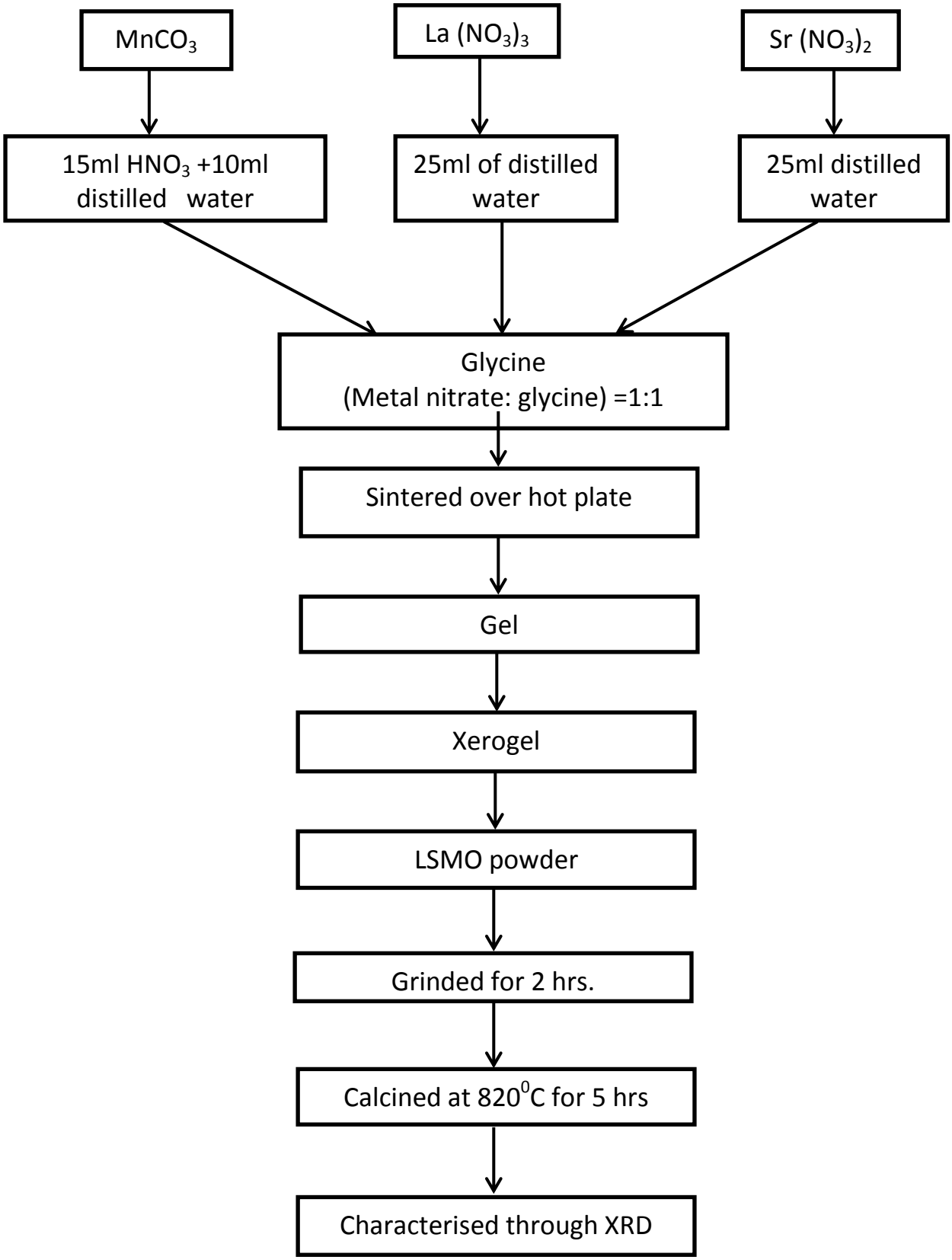

2.10 SUPERCONDUCTOR COMPOSITE OF BSCCO/LSMO

To obtain composite of BSCCO/LSMO we added x weight% of LSMO with (1-x) weight% of BSCCO (where x=5 & 10) and then grinded in an agate mortar for 1 hrs. , for mixing in atomic level. The sample is then pressed into pellet of 12mm diameter and ~1mm thickness by dry pressing method and then put in furnace for sintering at 800^0C for 1 hrs. Then the sintered pellet of the composite is taken out for the various characterisations

The main objective of the present studies is –

- Studying the effect of LSMO addition on the microstructural and variation of critical temperature (T_c) of BSCCO/LSMO nano composite.
- Comparative study of microstructural and critical temperature deviation with different composition of LSMO with BSCCO.

Two composition of (1-x) wt% of BSCCO: (x) wt%LSMO composites (where x=5,10wt %) have been synthesised by solid state synthesis process. Different characterisation such as XRD, SEM, EDXS, and R-T has been performed and the results are discussed in the following sections.

2.11 CHARACTERIZATION TECHNIQUE

2.11.1 RESISTIVITY MEASURMENT METHODS

Resistivity depends upon the nature of the material. The resistivity is calculated by measuring resistance R and the dimension of the sample (length, width, thickness etc.) The resistance is determined by voltage –current value. When a current of none value is fed to the sample, then the potential difference is produced in the voltage probe via point contact. From these measurements the resistivity is calculated as,

$$\rho = \frac{R \times A}{l}$$

There are various methods of resistivity measurements

(a)Two probe method

The test specimen for the two probe method may be in the form of strip, rod or bar. In two probe method only one pair of leads runs to the sample from RT instrument, in which case the voltmeter and current source share the same pair of leads.

In this case, $V= (I-I_1) (R_{sample}+2R_{contancts}+2R_{lead})-I_1(2r_{lead})$

Where, I is the transport current supplied by the current source, I_1 is the current through the voltmeter. Since the internal resistance of voltmeter is very high ($\sim 10^7\Omega$) than the other resistance in the circuit. Therefore, $I_1 << I$,

$$V=I (R_{sample}+2R_{contancts}+2R_{lead}).$$

So we cannot get the exact resistance by this method.

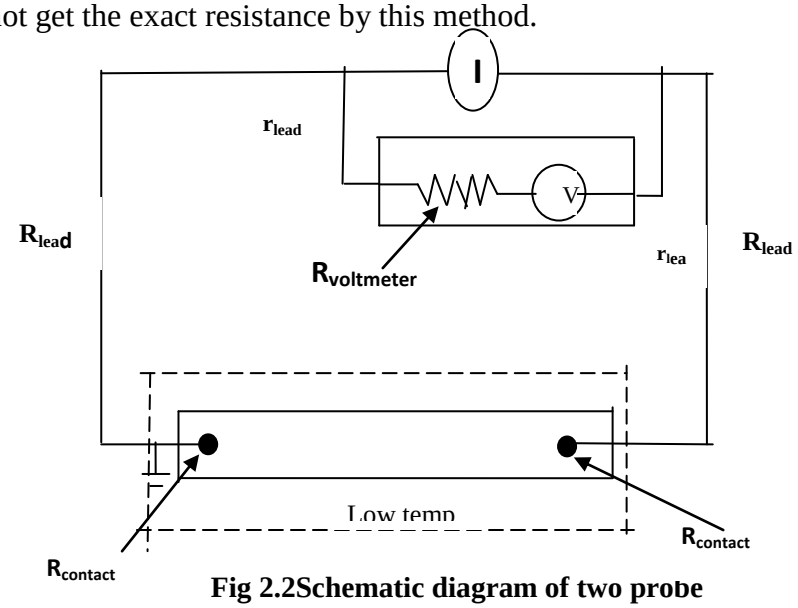

Fig 2.2Schematic diagram of two probe

(b) Four probe method

The advantage of for four probe method over two probe method that it minimizes the other contributions. i.e., lead resistance, contact resistance, etc. to the resistance measurement, which results an accurate measurement of sample resistance. In this method four equally spaced probes are in contact with a material of unknown resistance. The outer two probes are used for sourcing the current and two inner probers are used for measuring the resulting voltage drop across the surface of the sample.

In this case, the voltage, $V= (I-I_1) (R_{sample}) - I (2r_{contact}+2r_{lead})$.

As R_{volt} is typically much larger than other resistance in the circuit. Therefore, $I_1<<<I$.

$$So, V=IR_{sample}$$

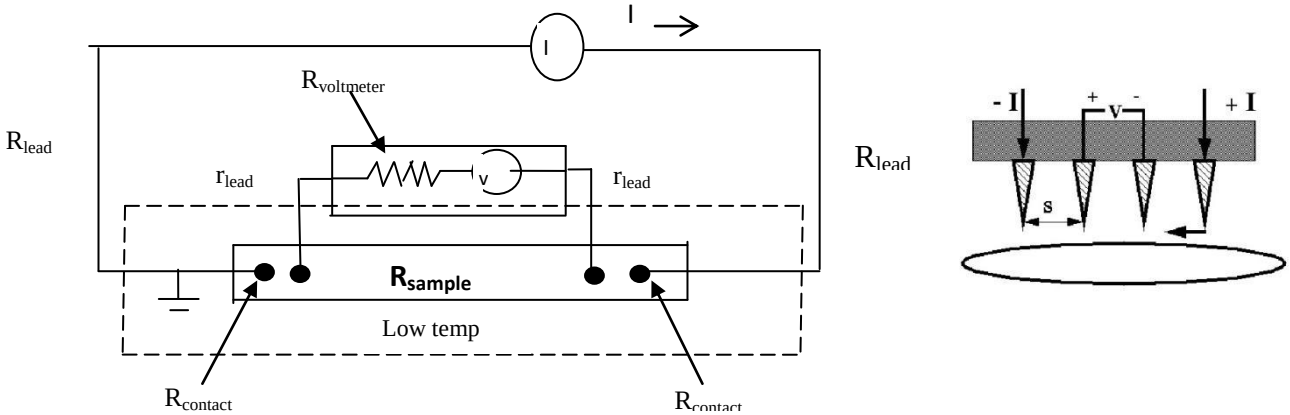

Fig 2.3Schematic diagram of four probe

(c)Van der Pauw method

This technique is commonly used for measuring sheet resistance of a material. For samples of irregular shape and size, the two and four probe method is not applicable and so choice is Van der Pauw method. This method includes the measurement of two resistances, R_A and R_B as shown in Figure given below.

$$R_A=V_{43}/I_{12}$$
$$R_B=V_{14}/I_{23}$$

The sheet resistance is related to this calculated resistance by the van der pauw formula,

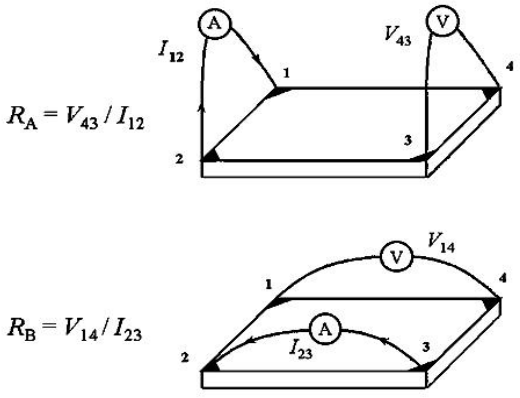

Fig 2.4 Van-der Pauw measurement in different configurations

$$e^{\frac{-\prod R_A}{R_S}} + e^{\frac{-\prod R_B}{R_S}} = 1$$

Where, R_s is sheet resistance to be determined .If R_A and R_B are similar, then resistivity is given by

$$\rho = \frac{\prod d}{\ln 2} \frac{(R_A + R_B)}{2}$$

Where, d is the thickness of the sample .If R_A and R_B are not similar, then resistivity is given by

$$\rho = \frac{\prod d}{\ln 2} \frac{(R_A + R_B)}{2} f\left(\frac{R_A}{R_B}\right)$$

Where $f(\frac{R_A}{R_B})$ is the function of the ratio $\frac{R_A}{R_B}$ only.

CHAPTER- 3

RESULTS AND DISCUSSION

3.1 XRD ANALYSIS

Phase analysis is done using the room temperature powder X-ray diffraction (Model: PW1830diffractometer, Philips, Netherland) with filtered 1.54 Å Cu Kα radiation. The samples are scanned in continuous mode from 20^0-80^0 with a scanning rate of 2^0/minute. The XRD pattern of the parent sample BSCCO (Pellet) sintered at 880^0C for 12 hrs and the substituent sample LSMO (powder) sintered at 820^0C for 5 hrs is shown in figure 3.1and 3.2 respectively. The sharp and well defined single diffraction peaks, which are different from those of the precursors, confirm the presence of single phase of BSCCO and LSMO. The observed XRD pattern matches with the standard XRD pattern of BSCCO (ICDD-460545) and LSMO (ICDD-401100). Indexing of XRD pattern is done by comparing the pattern and peaks to the standard JCPDS database. The best agreement between the observed inter planer spacing and Braggs angle with the calculated one, suggests tetragonal for BSCCO (a =3.82A^0, b = 3.82A^0& c =30.60A^0) and Monoclinic for LSMO (a =5.48A^0, b =5.53A^0 & c =7.79A^0). The XRD plot of 5wt% and 10wt% LSMO added BSCCO are shown in figure 3.3 and 3.4 respectively. The result indicates that on doping the structure of the BSCCO does not change and the major peaks still corresponds to the 2212 phase. Similarly, the XRD results of LSMO shows single phase and no other phases are seen. Besides these prominent peaks, some other peaks of low intensity at 25^0,43^0,46^0 angles are also observed, which do not belong to either of them and hence considered as impurity

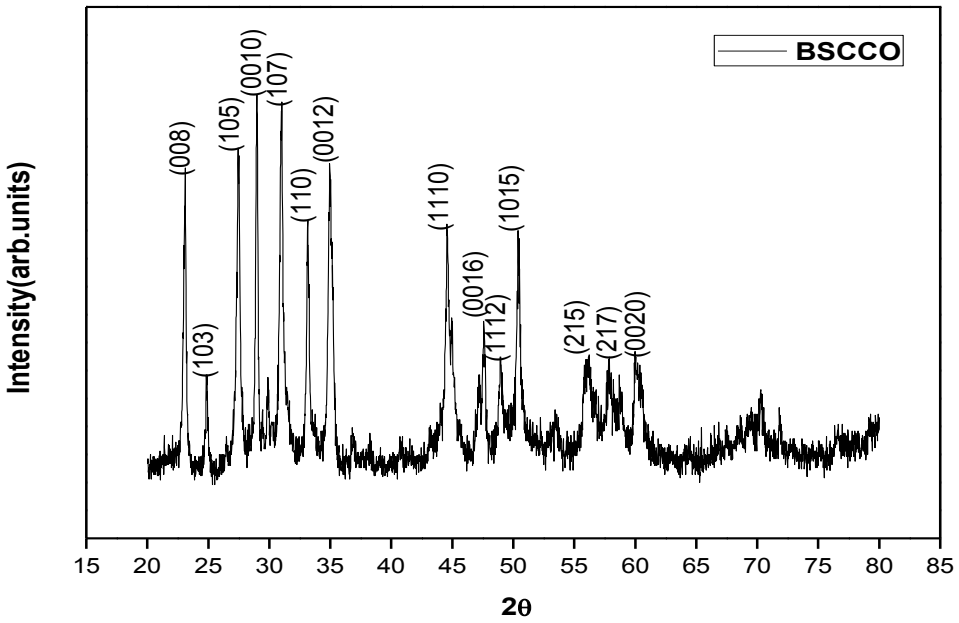

Fig3.1 X-Ray diffraction pattern of BSCCO

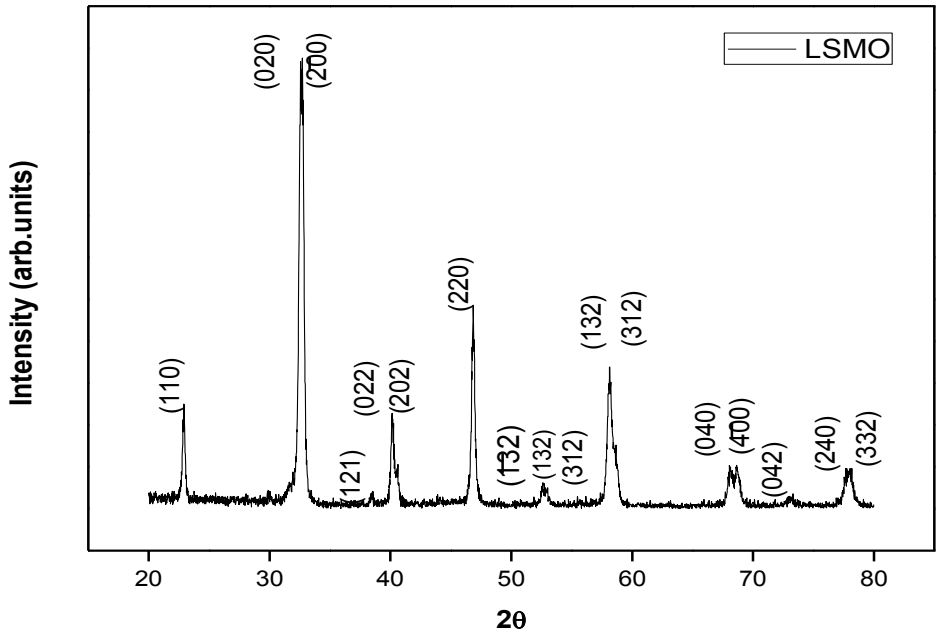

Fig3.2X-ray Diffraction pattern of LSMO

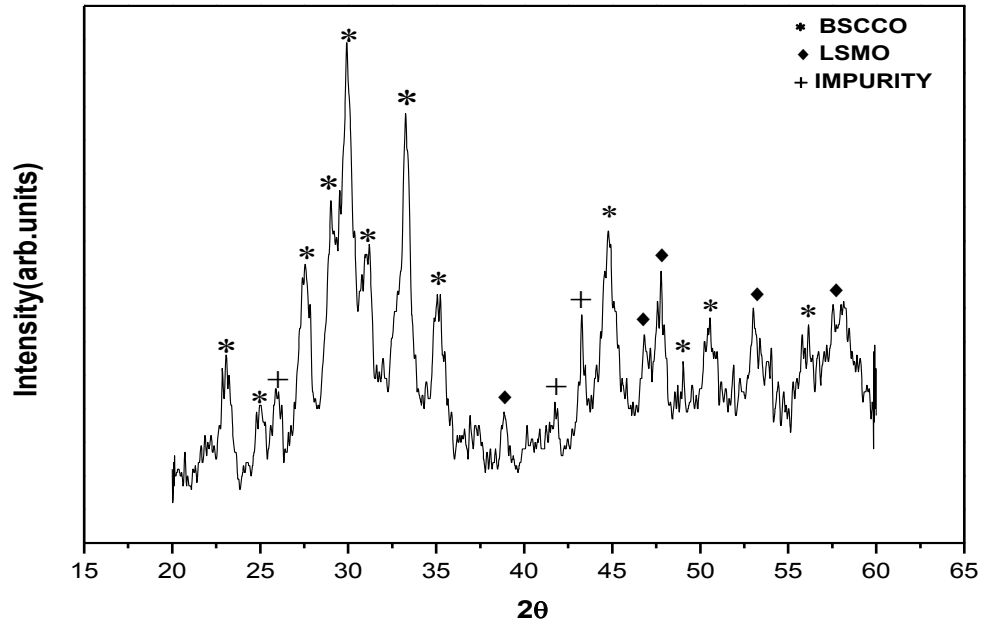

Fig3.3 X-ray diffraction pattern of BSCCO with 5wt% of LSMO.

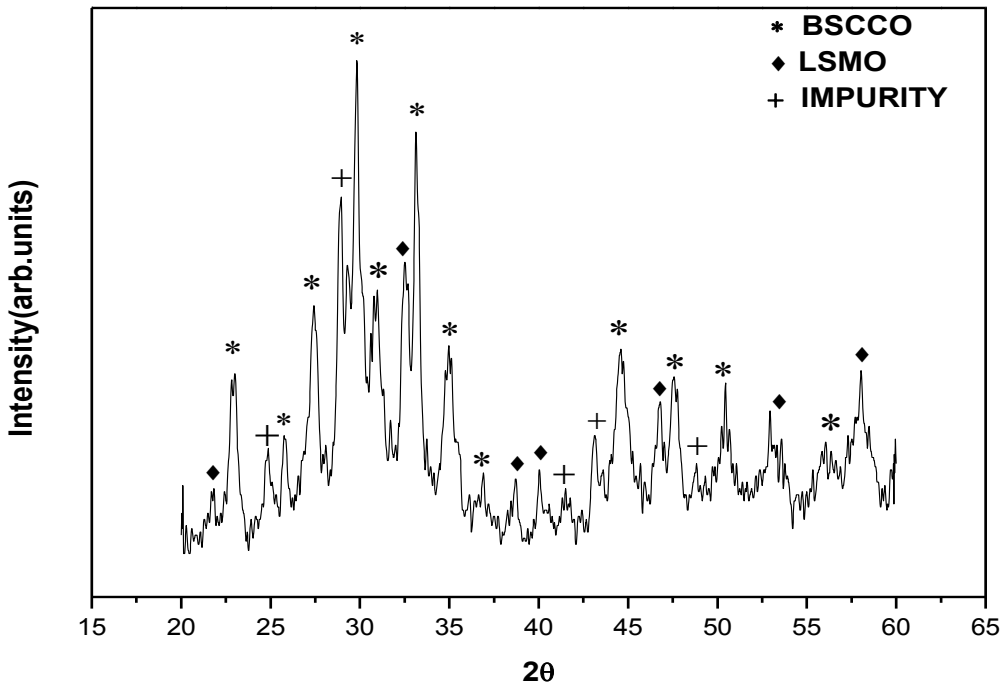

Fig 3.4 X-ray diffraction pattern of BSCCO with 10wt% of LSMO

3.2 SEM ANALYSIS

Microstructural features are studied using Scanning Electron Microscope (JSM 6480LV JEOL, Japan). Fig (3.5-3.7) shows the SEM image of the surface morphology of the samples (x 0wt%, 5wt%, 10wt %) respectively. The LSMO free $Bi_2Sr_2Ca_1Cu_2O_8$ sample consists of flake type grains and some needle type grains as shown in figure 3.5. The grains are distributed randomly or we can say that the grains in the specimen are oriented anisotropically and poorly connected. For the 5wt% and 10 wt% doped LSMO shown in fig. 3.6 and fig. 3.7, with a slight different microstructure, which probably due to composition shift. The grain size of the 5% sample decreases and which shows further decrease in grain size with 10wt% addition of LSMO. We observed the white space in the 5wt% and 10wt% doped LSMO sample. We have seen more white space in 10wt% doped sample than the 5wt% doped sample, which indicates the presence of LSMO. As LSMO shows the half metallic behaviour, so it is not a perfect conductor, therefore the electron beam does not pass through this region, so the white region are observed. It is also indicated that with the addition of different composition of LSMO the region of needle like grains and their orientation decrease with granular precipitation on the mother grain. These grains are disconnected as a result of the presence of minor impurity. This feature is observed by Mangapathi et.al. [50] With the Pb doping.

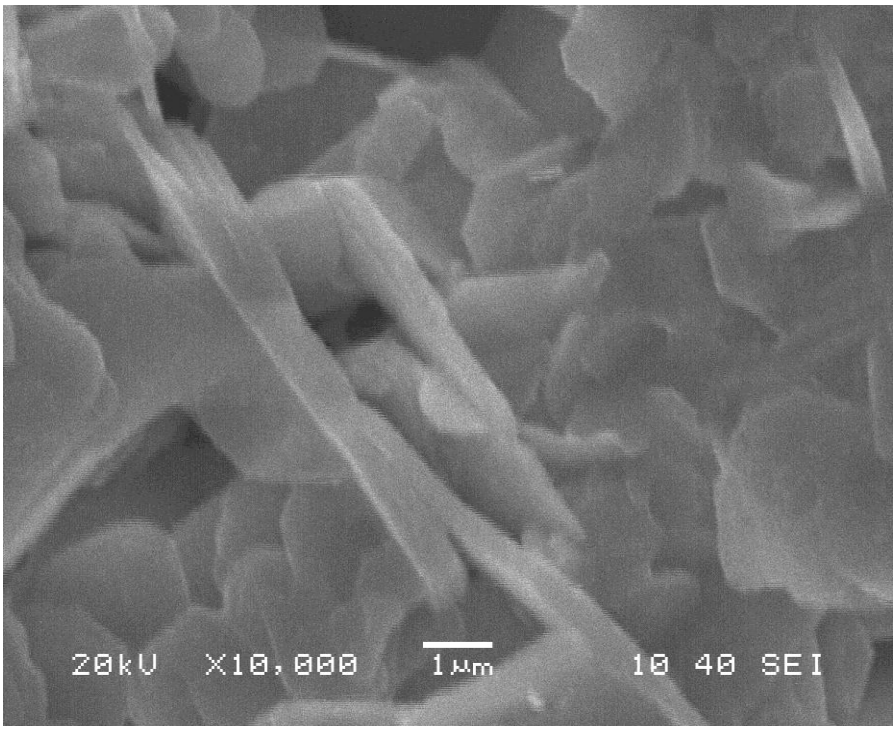

Fig3.5 SEM micrograph of BSCCO

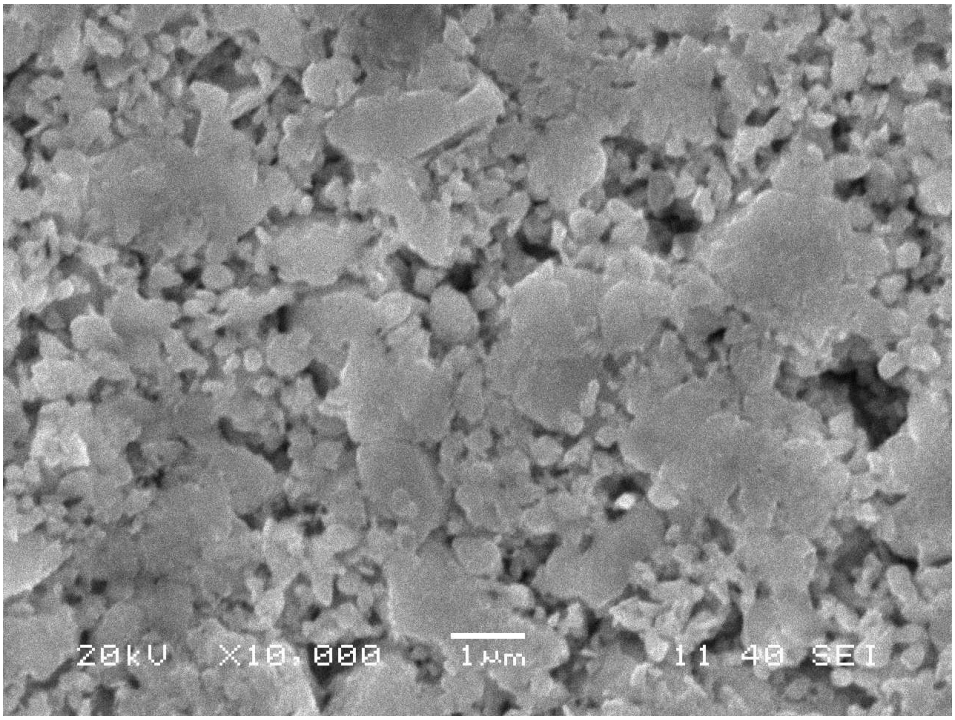

Fig3.6 SEM micrograph of 5wt%LSMO added BSCCO

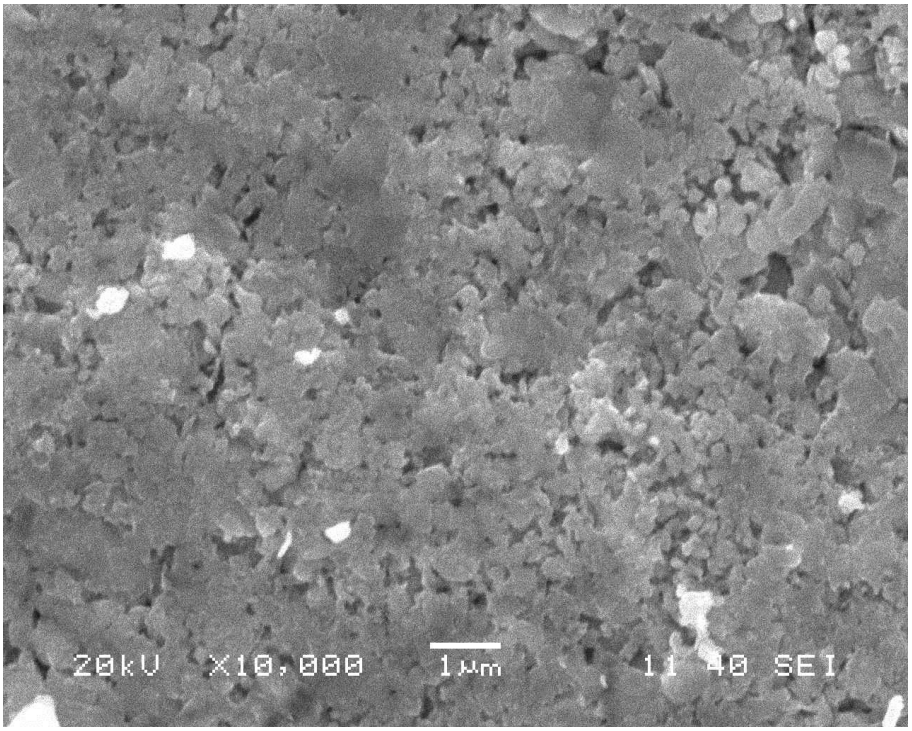

Fig3.7 SEM micrograph of 10wt%LSMO added BSCCO

3.3 EDXS ANALYSIS

The energy dispersive X-ray spectrometer (EDXS) of the BSCCO and 5wt% and 10wt% LSMO added BSCCO is shown in the following figures(3.8-3.10). EDX analysis is used to know the composition of the starting element in the sample. The EDX plot revels no extra peaks and reflects the presence of all the contituents. All the samples show the exact match for standard peak position for Bi, Sr, Ca, Cu, La and oxygen(O). This reveals that the elemental composition of all the samples do not contain any foreign element.It is odserved from the graph that with the addition of 10wt% LSMO with BSCCO the no of peaks of different composition , as well as the the peak hight increases.

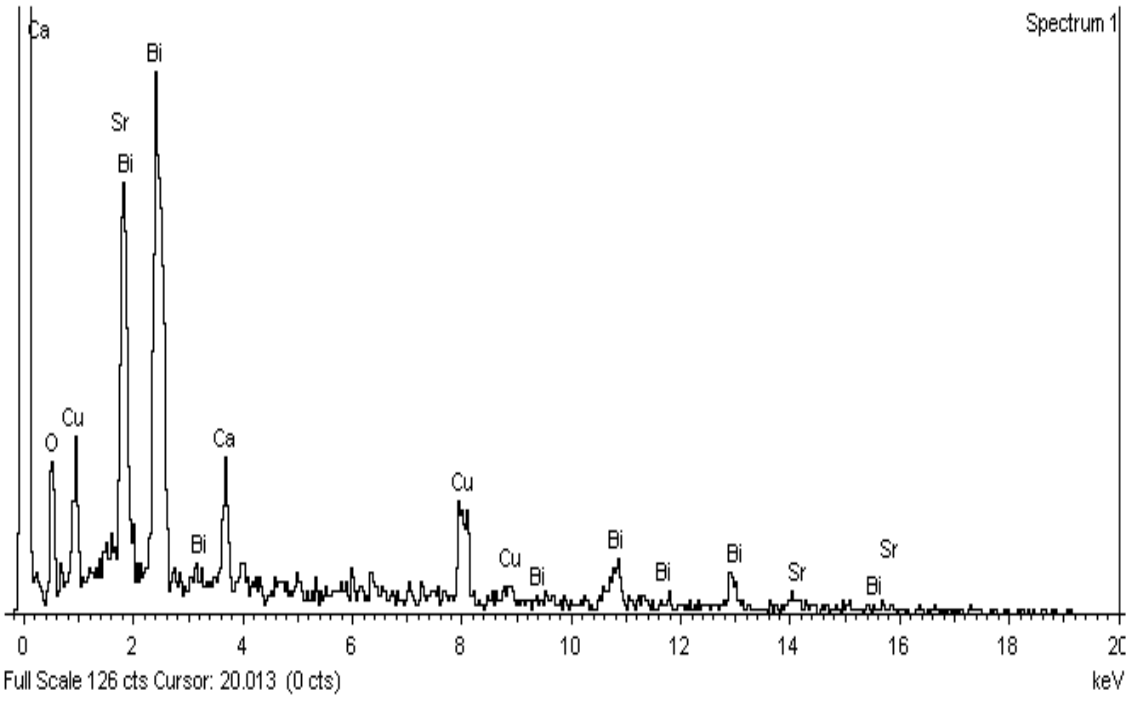

Fig3.8 EDXS image of BSCCO

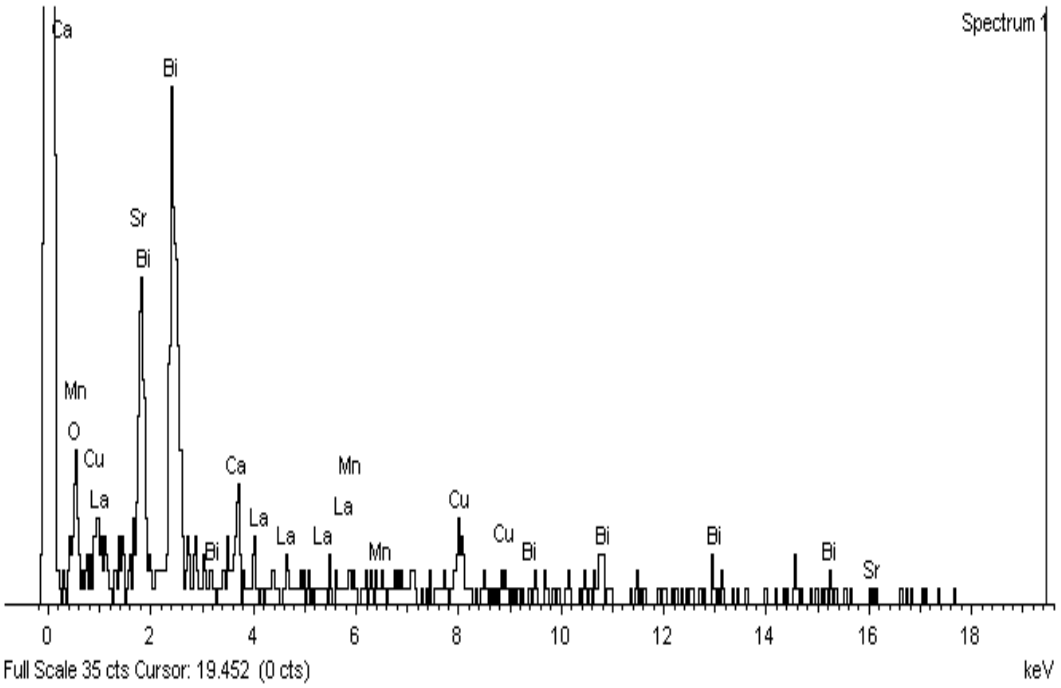

Fig 3.9 EDXS image of 5wt%LSMO added BSCCO

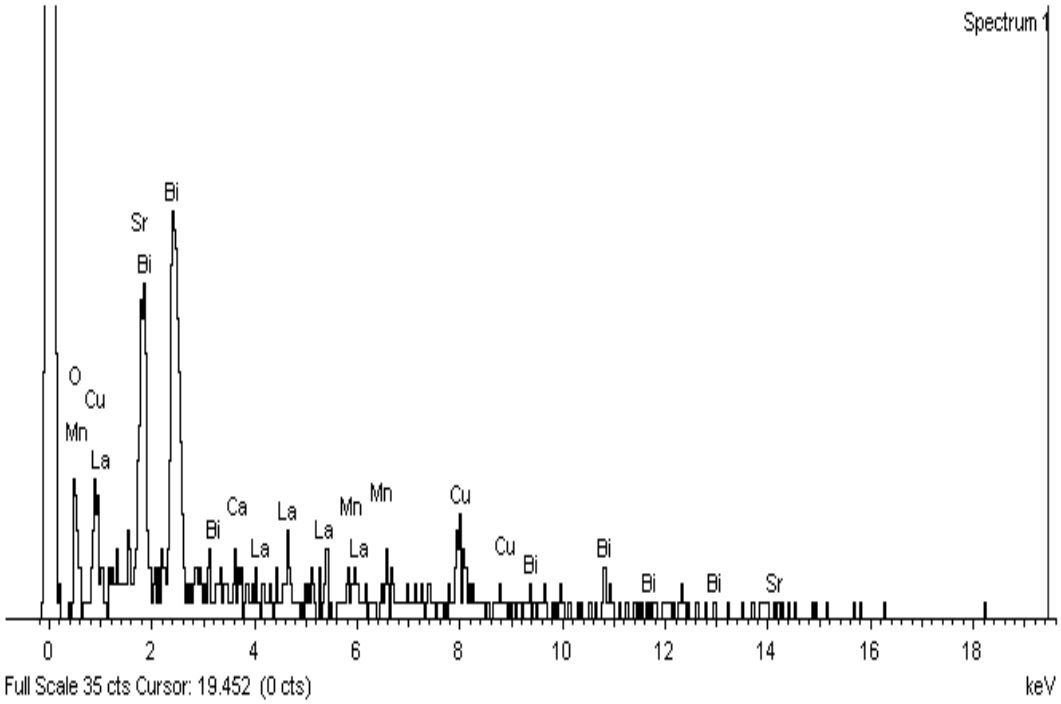

Fig 3.10 EDXS image of 10wt%LSMO added BSCCO

3.4 RESISTIVITY vs TEMPERATURE ANALYSIS

Resistivity vs.Temperature measurements of all samples are carried out using four probe arrangement, as it is one of the standard method for the measurement of resistivity. The temperature dependence of resistivity is measured using standard four probe technique with a nano volt meter (2182A-Keithley), current source (6221-Keithley), temperature controller (model 331S) and closed cycle refrigerator(Janis). We calculate the resistivity using four probe method and van der pauw method as discussed in chapter 2. For taking the measurement, the sample is mounted in cryocooler setup, then four probes are electrically connected to the sample by highly conducting silver paste.

The electrical resistivity versus temperature curve for all the sample, from 300K (room temperature) down to 8K for different compositions (i.e.x = 0wt%, 5wt%, 10wt%) are shown in the respective figures(3.11-3.13). It is found that all the samples show metallic behaviour above the $T_{c\text{-}onset}$ value. $T_{c\text{-}onset}$ transition temperature of three different samples are found to be about 78.97K, 66.73K, 60.83K respectively. The phase transition of BSCCO from normal metallic state to superconducting state happens at temperature 74.90K, 52.11Kand 30.79K respectively for BSCCO, 5wt% and 10wt% composition calculated from the first order derivative plot. This temperature is called critical temperature. It is also observed from fig(3.12) and fig(3.13) that with the addition of LSMO in the BSCCO, the transition temperature decreases gradually. The width of the transition marks the disorderness in the system. The width of the trantition temperature ($T_{c\text{-}onset} - T_c$) is plotted against increasing LSMO %. It is observed that the sharpness of the transition decreases and it become wider. This indicates the disorderess with increase in the concentration of LSMO (Fig-3.14).

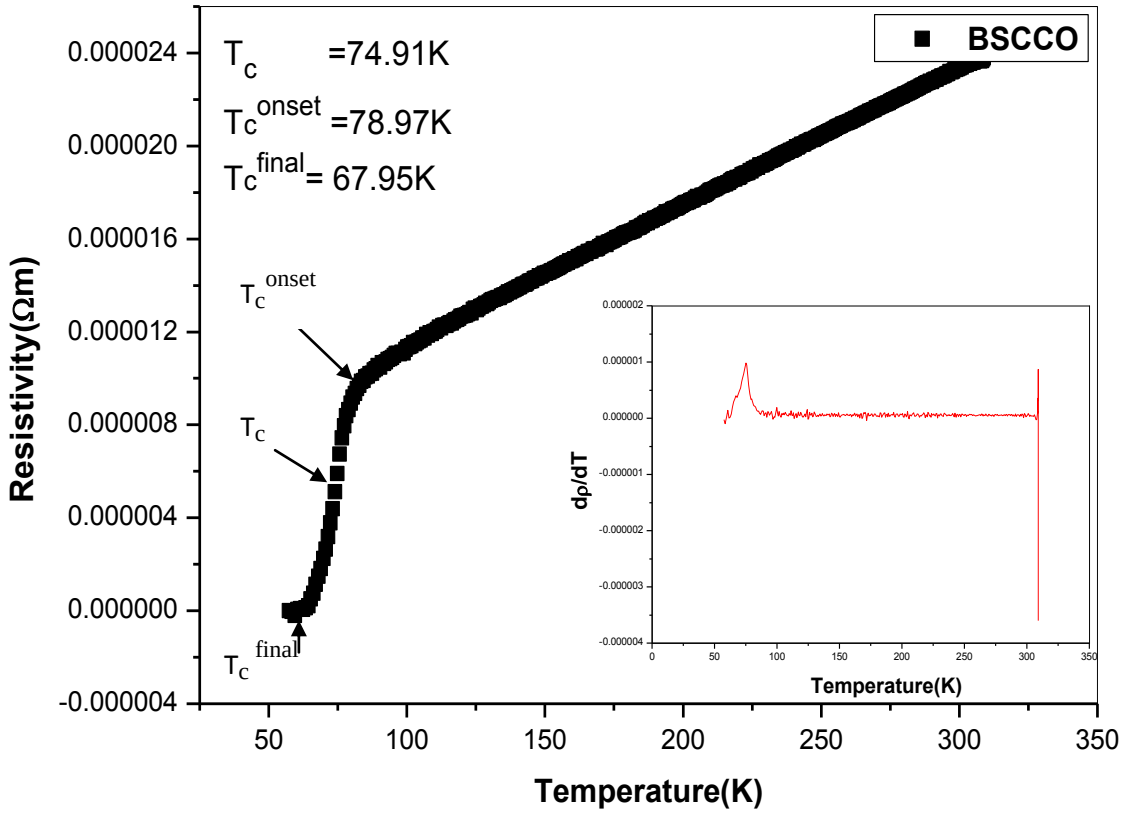

Fig 3.11 Resistivity dependent Temperature graph of BSCCO

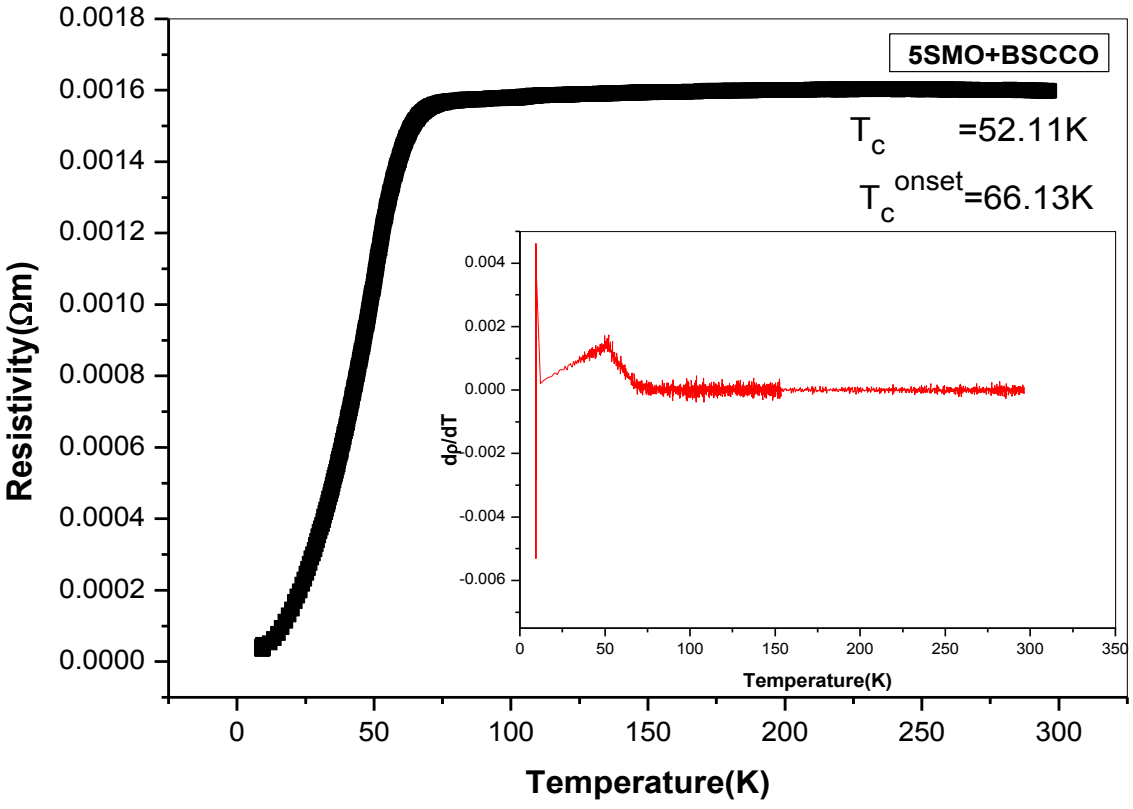

Fig 3.12 Resistivity dependence Temperature graph of 5 wt%LSMO added BSCCO

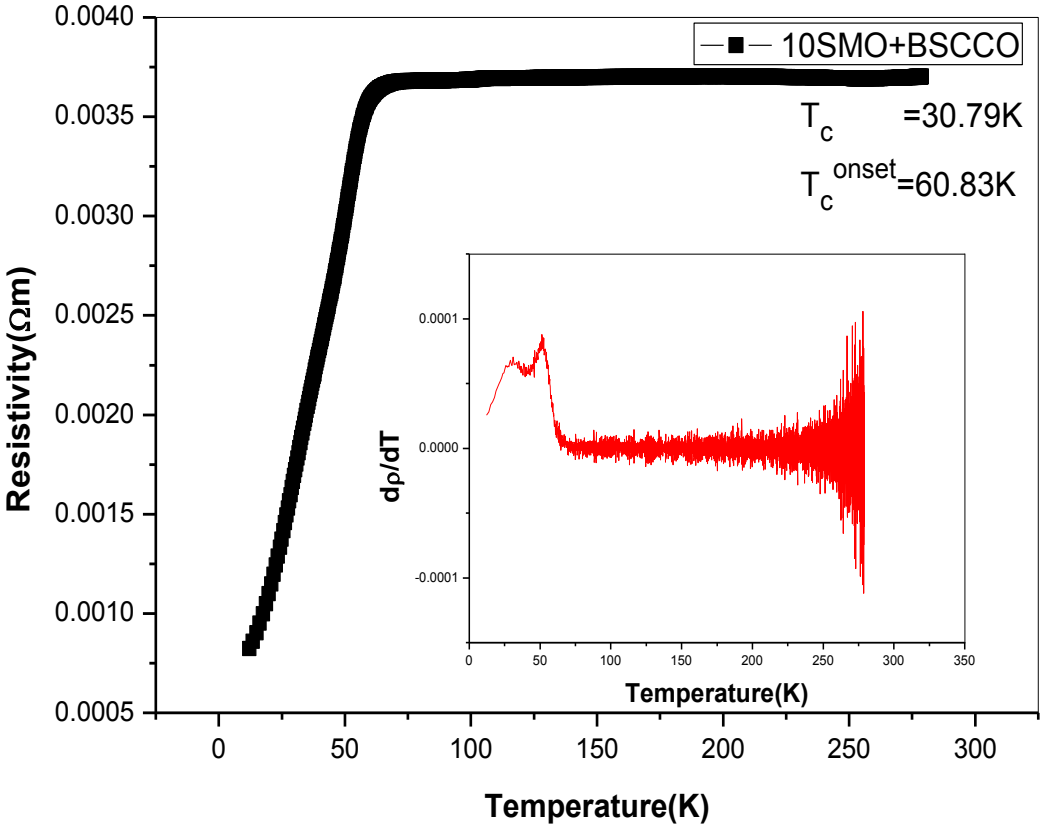

Fig3.13Resistivity dependenceTemperature graph of 10wt%LSMO addedBSCCO

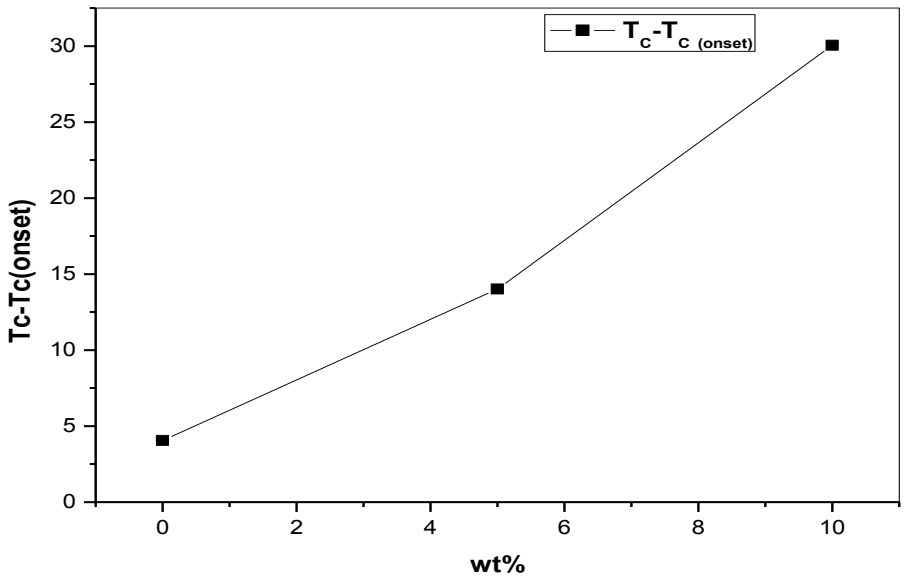

Fig 3.14 Difference in temperature with different wt% of LSMO added with BSCCO

CHAPTER- 4

Conclusion

The sample BSCCO/LSMO is prepared successfully. BSCCO ($Bi_2Sr_2Ca_1Cu_2O_8$) is prepared by solid state synthesis route and LSMO ($La_{0.85}Sr_{0.15}MnO_3$) is prepared by sol-gel route. The x-ray diffraction shows sharp and well defined peaks are for BSCCO, LSMO and their composites. On comparing the x-ray diffraction results to JCPDS database, the structure of BSCCO is found to be tetragonal having a=b =3.82 Å and c=30.60 Å and monoclinic for LSMO having a=5.48Å, b=5.53 Å and c=7.79 Å.

From the SEM study of LSMO added BSCCO the presence of rounded shaped LSMO having small grain size is observed in needle shaped BSCCO. The decrement in grain size was observed. Also from the SEM image the conducting and non-conducting behaviour of BSCCO and LSMO respectively was confirmed from the colour of the image. The orientation of the grains decreases with granular precipitation in the parent sample with addition of different composition of LSMO. EDXS plot revels no extra peaks related to elements other than the constituents. It is also observed from the EDXS graph that with the addition of 10wt% LSMO with BSCCO the no of peaks of different composition increases and peak hight also increases.

From resistivity vs. temperature measurement, the superconducting transition temperature T_c of the parent BSCCO is found to be 74.91K, observed from the sharp first order derivative peak. With increase in concentration of LSMO in BSCCO the transition temperature decreases to 52.11K and 30.79K for 5% & 10% (by weight) respectively. For 10% sample, one extra peak in the derivative plot is seen at 51K, suggesting more than one superconducting phases. Since LSMO is in ferromagnetic state below 75K, the inclusion of ferromagnetic material decreases the superconducting properties of parent BSCCO [2]. The width of the transition marks the disorderness in the system. The width of the trantition temperature ($T_{c\text{-onset}} - T_c$) is plotted against increasing LSMO %. It is observed that the sharpness of the transition peak is decreases and it become wider,this indicates the disorderess with increase in the concentration of LSMO .

REFERENCES

[1] http://www.wordiq.com/definition/Superconductivity

[2] Charles Kittel, *Introduction to solid state physics*, Seventh edition, Wiley India, 2004

[3] R.K.Puri, V.K.Babbar, *Solid state physics*, S.chand, 2009

[4] S.O.Pillai, *Solid state physics*, 6th edition, new age international publishers, 2006

[5] Superconductivity www.wikipedia.com

[6] BCS theory www.wikipedia.com

[7] Coherence length www.wikipedia.com

[8] hyperphysics.phy-astr.gsu.edu/hbase/solids/scond.html

[9] Liz Prettner, High Temperature Superconductivity February 17, 2010

[10] Lanthanum Barium cooper oxide www.wikipedia.com

[11] David M. Friedman, New research on YBCO superconductor.

[12] BSCCO www.wikipedia.com

[13] Narlikar, A.V; High temperature superconductivity, *Springer*, Berlin, P.35 2004.

[14] J.X.Jin*, S.X.Dou and C.Cook, Engineering application of high T_c superconductors.

[15] Superconducting Terminology and the naming scheme by, *SC Links from NSTA*.

[16] Sotelo A, Pena JI et.al. Synthesis of the $Bi_2Sr_2CaCu_2O_{8+\delta}$ superconductor, *Journal of Materials Science* **32** 5679-5685(1997).

[17] Z.Meric et.al. C-axis tunnelling of round mesas in high temperature superconductors for terahertz emission.

[18] Pavel E.Kazin and Yurin .Tretyakov Nano structured oxide superconductors.

[19] Hiroki sasakura et.al. *IEEE Transactions on Applied superconductivity*, Vol **9**, No.2, june1999.

[20] Alibiss, B.A; I.M; Obaidat et.al. *Solid state communications,* Vol1 **50**, p.1542-1547, sept2010.

[21] Berdan ozkurt, *Journal of Superconductivity and Novel magnetism* 2012.

[22] Lattice defects and flux pinning in crystallized metal oxide glasses in the Bi-Sr-Ca-Cu-O system. *Applied physics Letters* /Volume **55**.

[23] Pavel E.Kazin and YuriD.Trethakov, Nanostructured oxide superconductors.

[24] H.Nadifi et.al.*Superconducting.sci.Technology* **13**, 1174-1179(2000)

[25] M.Ochsenkiihn-petropula et.al.*Journal of Thermal analysis*, Vol**52**, 903-914(1998)

[26] S.Sengupta, L.R.Motowidlo, R.R.Garcia et.al. *IEEE Transactions* on applied superconductivity, Vol.**9**, No2, June 1999

[27] J.Bock et.al. *Solid state communication*, Vol.**72**, No-5, P.453-458, 1989.

[28] H.OESTERREICHER et.al. , *Materials Letters,* Vol-**6**.No.-8, 9, 1988

[29] EmanuelI.Cooper et.al. *Materials Letters*, Volume-**7**, No.1, 2, 1988.

[30] S.C.Bhargava, J.S.chakrabarty et.al, *Solid state communications*, vol.**78**, No. 5, pp.397-401, 1991.

[31] Ashok pandey, *Biochemical Engineering Journal* **13**, 81-84(2003)

[32] Advantages of Solid-state relays over Electro mechanical relays, application note AN-145, www.clare.com

[33] Asthana, A. K. Nigam and D. Bahadur, *Phys. Stat. Sol. B*, **243,** 1922–1928 (2006).

[34] W.J. Lu, Y.P. Sun, X.B. Zhu, W.H. Song and J.J. Du, *Maters. Letters*, **60**, 3207 (2006).

[35] S. Jin, T.H. Tietel, M. McCormack, R.A. Fastnacht, R. Ramesh and L.H.Chen, Sci., 264, 413 (1994).

[36] M.B. Salamon and M. Jaime, *Rev. Mod. Phys.,* **73**, 583 (2001).

[37] Banach, G et.al. *Journal of magnetism and magnetic materials,* Volume-**272**, P.1963-1964.

[38] Vstrbik et.al. *Journal of physics*, conference series 223 (2010).

[39] LSMO www.wikipedia.com

[40] Mara Jose Calderon Prieto., Magnetic and Electric properties of system with colossal magnetoresistance, may, 2001

[41] www.leroy-somer.com/documentation-pdf/depliants/3800a-en.pdf

[42] Sangeeta N.Kule et.al, ceramic doping and stochiometry control for biomedical use of La0.7Sr0.3MnO3 nanoparticles, *Science direct*, volume-**2**, issue-4, pages 217-221, 2006

[43] A.Urushibara et.al, Insulator- metal transition and giant magnetoresistance in La1-xSrxMnO3, *Physical review B*, volume-**51**, number-20, 1995.

[44] Javier Bermejo et.al, Spin relaxation in nanophased manganites, *Journal of Non-crystalline solids* **354**, 5258-5260, (2008).

[45] D.Grossin and J.G.Noudem, Synthesis of fine La0.8Sr0.2MnO3 powder by different ways, *Elsevier Science*, **6** 939-944, (2004)

[46] J.M.Liu et.al, Oxygen deficiency activated anamolous transport in La2/3Sr1/3MnO3 thin films deposited by Laser ablation, *J.Phys: condens. Matter* **14**, 3167-3173, (2002)

[47] Donald T.Morelli et.al, Magnetocaloric properties of dopped Lanthanum Manganite films, *American Institute of Physics* (S0021-8979(96)09101-7), 1996

[48] M.Pekala et.al, *Magnetocaloric and magnetic materials*, volume-**322**, issue-21, pages 3460-3463, 2010.

[49] L.Pinsard et.al, Structural phase diagram of La1-xSrxMnO3 for low Sr dopping, *Journal of Alloys and compounds*, 262-263, 152-156. (1997)

[50] D.mangapathi Rao, T.somaiah et.al.*Crys.Res.Technol*, **28**, P.285-298(1993).